ROBUST POWER SYSTEM SECURITY ASSESSMENT AGAINST UNCERTAINTIES

（不確定環境における電力システムのロバスト信頼度評価）

A Dissertation by

MUHAMMAD ABDILLAH

Graduate School of Engineering
Department of System Cybernetics
Hiroshima University

Submitted in partial fulfillment of the requirements for the degree of Doctor of Engineering

September, 2017

ABSTRACT

In recent years, most countries are introducing renewable energy (RE) as an alternative energy resource instead of the conventional power plants. The foremost types of renewable energy resources widely employed in the world are photovoltaic (PV) and wind power. However, the quick development of large scale RE generation and its integration to power system grid lead to severe problems relating to the reliability of power system network. Especially, uncertainties and intermittency of RE outputs threaten the power system security. The increase in RE implies reduced controllable resources which make system security problem critical. Therefore, it is important to evaluate the robustness of the system controllability in order to preserve system security against uncertainties of RE outputs. In this thesis, the robustness of the system in this context is referred to as "Robust Power System Security." Two types of security regions for static operating point and dynamic transition of system operation are defined, which are Robust Static Security (RSS) and Robust Dynamic Feasible (RDF) regions, respectively. The thesis is summarized as follows:

Chapter 1 presents the background of this research, the impact of uncertainties of RE, types of disturbances on power system security. Then, the proposed approaches are outlined.

Chapter 2 describes basic concept and definition of power system security, including a brief overview of conventional methods. The concept of Robust Power System Security dealing with uncertainties is described as an introduction to the following chapters.

Chapter 3 presents a new approach for RSS problem applied to static economic dispatch. The proposed method is to obtain upper and lower bounds of security region. The difference between the bounds indicates the diameter of security region, which can be used as a security measure. Linear programming (LP) is employed to solve the RSS problem. The effectiveness of the proposed method is demonstrated taking into account uncertainties of PV generations.

Chapter 4 provides the extension of RSS problem. In order to measure the security region in dynamic power system operation circumstances, RDF area is defined. A bi-level optimization problem is formulated to monitor RDF region. Then, the problem is

linearized and transformed into mixed integer linear programming (MILP) problem, which can be effectively solved. The proposed approach is demonstrated using six-bus, IEEE 14-bus, IEEE 30-bus, and IEEE 118-bus standard models taking into account all dynamic factors in power system operation. It is shown that the method clearly indicates dangerous operating hours in a 24-hour system operation.

Chapter 5 presents the resume of the major achievements. Further, the future research works are discussed in relation to the thesis.

ACKNOWLEDGEMENT

First and foremost, praise to Allah for his kindness for giving me the strength, knowledge, ability and opportunity to undertake this Dissertation Thesis and to persevere and complete it satisfactorily. Without his blessings, this achievement would not have been possible.

I really appreciate the kindness of my supervisor Professor Naoto Yorino for his invaluable suggestion, excellent guidance, motivation, patience, comments, and professional support during my study in Hiroshima University. His guidance in performing research work and writing the thesis and the publications is extremely helpful. Besides his technical support, I have benefit from him positively in my personal live. I would like to express my greatest gratitude to all members of EPESL laboratory, especially Prof. Yoshifumi Zoka and Prof. Yutaka Sasaki for encouraging my research step by step as well as living in Japan. I would also like to thank committee members, Prof. Katsuhiko Takahashi and Prof. Ichiro Nishizaki for serving as board members even at hardship. Thank you very much for your brilliant comments and suggestions. Last but not the least, I would like to thank my family: my wife Rida Farida, my parents, my brothers, my sisters, and my friends for supporting me spiritually throughout my life.

Muhammad Abdillah

2017

TABLE OF CONTENTS

LIST OF FIGURES

LIST OF TABLES

NOMENCLATURE

Variables and Functions:

d	Diameter of upper and lower bounds of security region
$f^n(*)$	Power flow equations (equality constraints)
$g^n(*)$	Inequality constraints in power flow problem
$H(*)$	Power flow constraint set consisting of f^n and g^n *for all n*
$H_{DF}(*)$	Unified constraint set consisting of $H(*)$ and dynamic ramp rate constraints
$p=[P_{PV}, P_D]$	Uncertain parameter vector (uncontrollable)
P_D	Load (MW)
P_G	Output power of generators (MW)
P_{PV}	Output of photovoltaic generations (MW)
P_{slack}	Output of slack node generators (MW)
P_{TL}	Transmission line flow (MW)
$u=[P_G, P_{slack}]$	Control vector (node injection by generators)
x	Dependent variables (voltage vector)
δ	Maximum ramp-rate of generator

Parameters:

c	Normal vector for objective
e	Unit vector
n	Contingency number ($n = 0$ for normal condition, $n = 1, ..., N$ for contingencies)
N_B	The number of nodes
$\hat{p}(t \mid t_0)$	Estimation of p at t predicted at t_0
$S^{(n)}$	Transformation matrix from node injection to line flow for contingency n (DC power flow)
t	Time point (t_0 : base point, $t_0 < t$: future point)
$\bar{\Delta}(t \mid t_0)$	Maximum prediction error

$\overline{\Delta}_D(t \mid t_0)$	Maximum error for load forecast
$\overline{\Delta}_{PV}(t \mid t_0)$	Maximum error for PV forecast
$\overline{*}$, $\underline{*}$	Upper and lower bounds of variables $*$

Regions and Sets:

DF_u	Dynamic feasible region (Set of u)
R_p	Region of uncertain parameter p (Set of p)
RDF_u	Robust dynamic feasible region (Set of u)
RSS_u	Robust static security region (Set of u)
SS_u	Static security region in u space (Set of u)

Abbreviations:

CI	Confidence interval
CL	Confidence level
CPU	Central processing unit
LB	Lower bound
MILP	Mixed integer linear programming
PV	Photovoltaic
RE	Renewable energy
UB	Upper bound

CHAPTER 1 : INTRODUCTION

1.1. Research Background

Nowadays, the development of renewable energy (RE) technology as an alternative energy source is impressively increased in order to contribute to solving the world energy problems. However, the rapid development of high RE integration to power system network yields problem in electric power system operation. Photovoltaic (PV) generation as a type of renewable energy source in Japan is rapidly growing and endangering the power system network security as well as power quality. A suitable treatment for the uncertainties of PV output plays a key role in power system operation and planning. Continuous intermittency of PV generation output causes sudden changes of power in the power system network yielding uncertainty such as significant ramp effect. The influence of the increasing use of renewable energy technology requires mostly new methodologies for power system operation and planning. The power system operation and planning may face difficulty in the future related to unpredictable uncertainties which are significantly increased in the various power system. Notably, a power system security problem will be a critical matter in the operation planning as well as in real-time operation. The security criterion has been employed widely in the world to nurture power system reliability and security through various basic studies on the security control scheme. This scheme includes the use of computer program incorporated a security function to deal with operating conditions as well as disturbances [1], corrective and preventive security control evaluation for real-time operation [2], and predictive security assessment based on the concept of security corridor [3]. The security criterion is considered for power flow studies [4]-[10], and various approaches are contributing the scheme [11]-[13]. These methods are formulated in a deterministic approach and outrageously rely on the accuracy of load forecast and prediction of system circumstances. Hence, new measures as well as effective methods [14]-[17] are studied based on the extension of deterministic approaches. Furthermore, various studies on the system security issue have been performed related to contingency analysis. Contingency constrained power system optimizations have been proposed such as for optimal power flow [18], unit commitment problem [19] and transmission expansion [20]. Since various problems arise in power system planning and operations due to the rapid increase in REs, various trials and

methods have been proposed to take into account their uncertainties efficiently. Those researches include robust optimization for unit commitment and economic dispatch [21], [22], the computation of cautious operation planning and worst case scenario [23], [24], decision-making process [25], and stochastic security constraint unit commitment using energy storage system [26].

While such various approaches are being developed, the increase in uncertainties is being accelerated. Therefore, more direct assessment of the feasibility of system operations is being required. Power system flexibility is becoming an important subject in the evaluation of the maximum ranges of uncertainties without deteriorating power system reliability [27]-[29]. Based on this concept, the maximum ranges for REs are computed as do-not-exceed limit [30], [31]. There is a more direct evaluation of feasible region under uncertainties, such as the assessments of the dispatchable region of variable wind generation [32] and loadability sets [33]. A term "Robust Power System Security" in this thesis is defined and employed to maintain the robustness of the power system security criterion for all pre-specified uncertainty set [34], [35], where transient stability [36]-[38] is also analyzed to alert future power system operation and planning in Japan. The basic concept is that the uncertain events and disturbances are classified into two categories in line with their severity.

Acceptable disturbances/events: Their impact on a system is less than a critical level so that the system can be recovered within assumed payable cost.

The events in this category may be treated in a probabilistic manner, in which each risk is evaluated by its expected damage defined by the product of the expected cost and its probability. There have been various approaches proposed so far. Even though probabilities of such events are not always reliable for events which rarely occurred, the probabilistic methods are still effective in reducing the expected annual cost of power system operation.

Fatal disturbances/events: The impact is greater than the critical level and results in "fatal disaster." The losses exceed acceptable costs.

A typical situation for this event is that the cost is beyond evaluation and the probability is reasonably high. In such cases, the probabilistic approach, as well as the expected cost is not meaningful in reality. Special treatments are required for this event so that the fatal consequences are avoided. An example is that the N-1 contingencies are regarded as fatal disturbance managed by deterministic manner. Furthermore, the well-known N-k security criteria in industry practice are implemented as deterministic

approaches.

The latter events result in fatal consequences such as blackout, which must be avoided even if the probability is small. This thesis proposes the robust power system security where the security region as the feasibility region is defined in relating to the latter case. The proposed approach is similar to the flexibility in [39]-[43], while the main difference is that, instead of computing the maximum ranges of uncertainties, the operational feasibility in the space of control variables are measured for the pre-specified uncertainty set. A real-time unit commitment and economic dispatch approaches in [44] have been proposed where transmission overloadings are treated by stochastic power flow while the supply-demand balance is guaranteed by the computation of feasibility region [45], [46] for the maximum prediction errors and contingencies.

1.2 Study Objectives

The objective of this thesis is the development of a new formulation and method to evaluate the size of robust power system security region under uncertainties or specified prediction errors. The proposed approach is used to guarantee the power system operation and planning which takes into account uncertainties satisfying security criterion as depicted in Figure 1.1.

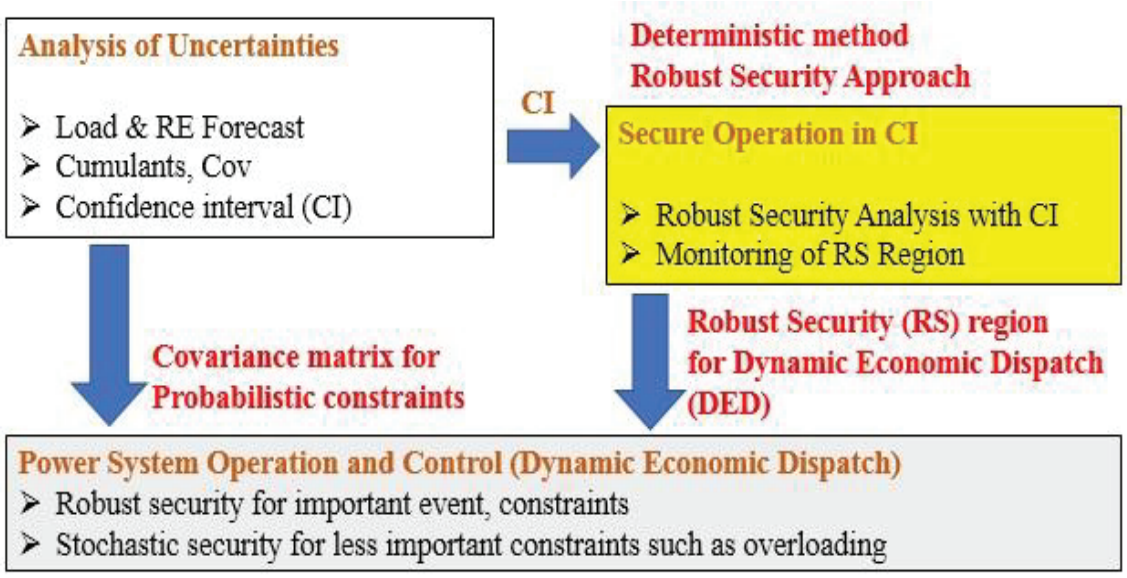

Figure 1.1. The scheme of robust power system security approach

Load and RE forecast data are obtained by conducting data analysis. Cumulants such as covariance matrix are used for probabilistic constraints in the power system operation and control. This thesis focuses on robust power system security approach

where confidence interval (CI) of the uncertain parameters is used to avoid the system collapse. Two types of security regions are defined for static operating point and dynamic transition of system operation, which are robust static security (RSS) and robust dynamic feasible (RDF) regions, respectively. The problem is constructed as a min-max optimization problem which is highly nonlinear and is hard to solve. Hence, the simplification of the problem is required for linear load dispatching problem.

The main contributions of this thesis are summarized as follow,

1. A novel formulation and method are presented to calculate the size of the worst case feasible region under dynamically varying prediction errors in system operation.
2. The approach is used to assess "Robust Power System Security" guaranteeing the security criterion, which is employed to the static and dynamic economic dispatch problems using DC power flow model.
3. When operation cost as objective function is selected, the method can evaluate the worst case economic operation planning, while measuring the size of feasibility region including infeasible cases.

1.3 Outline of the Thesis

The thesis is summarized in the following chapters:

Chapter 1

This chapter presents the background of this research, the impact of uncertainties of RE, types of disturbances on power system security. Then, the proposed approach is outlined.

Chapter 2

This chapter describes basic concept and definition of power system security, including a brief overview of conventional methods. The concept of Robust Power System Security to deal with uncertainties is described as an introduction to the following chapters.

Chapter 3

This chapter presents a new approach for RSS problem applied to static economic dispatch. The proposed method is to obtain upper and lower bounds of security region. The difference between the bounds indicates the diameter of security region, which can be used as a security measure. Linear programming (LP) is employed to solve the RSS

problem. The effectiveness of the proposed method is demonstrated taking into account uncertainties of PV generations.

Chapter 4

This chapter provides the extension of RSS problem. To measure the security region in dynamic power system operation circumstances, RDF region is defined. A bi-level optimization problem is formulated to monitor RDF region. Then, the problem is linearized and transformed into mixed integer linear programming (MILP) problem, which can be effectively solved. The proposed approach is demonstrated using six-bus, IEEE 14-bus, IEEE 30-bus, and IEEE 118-bus standard models taking into account all dynamic factors in power system operation. It is shown that the proposed method indicates dangerous operating hours in a 24-hour system operation.

Chapter 5

This chapter presents the resume of the major achievements. Further, the future research works are discussed concerning the thesis.

CHAPTER 2 : POWER SYSTEM SECURITY ISSUES

2.1. Conventional Method for Power System Security

Electricity is an indicator of social and economic development where it brings expediency to society. The primary objective of electric power system operation which consists of large, complex, and strongly connected equipment networks is to generate, transmit, and distribute electricity since the quality and preservation of electric energy supply are essential to satisfy customer demands such as household, industries, universities, and others. Therefore, security and reliability of power system operation are crucial in order to preserve power supply satisfying the customer demands. Reliability refers to the ability of electric power system that produces electricity and transfers it to customers within satisfied standards and in the amount desired. Two basic measurements such as frequency duration and magnitude of adverse effects on electric power are used as a reference to measure the system reliability. Reliability involves two concepts: adequacy and security. Adequacy is the ability of power generation units transferring the power through the transmission line in order to satisfy the electrical demand of the customers at all times. Security refers to the ability of the electric system to restrain from an incidental disruption. Security is the important issue in planning, design and operation stages of electric power system. Power system security is defined as the probability of the system operating point remaining within an acceptable range in normal condition or under sudden disturbance. In power system operation and planning, operating system point must frequently be observed in order to investigate the existence of a critical condition or vice versa. The operating state of the power system can be classified into many states. The security state is crucial as a reference to support the decision making by a system operator. Security state of power operation is decomposed into three states as follows [47]:

1. Preventive (Normal) State

   The system operation is in a preventive/normal state when power supply satisfies electrical demands of all customers at a standard frequency and desired voltage. The control objective in the preventive state is to meet the customer demands continuously without interruption.

2. Emergency State

   The system operation exists in the emergency state when power supply satisfies all the customer loads, and there is violation regarding one or more constraints such as the voltage at a customer cannot be preserved at a safe minimum. The control objective of the emergency state is to alleviate the system distress and prevent further degradation while fulfilling a maximum of customer demand.

3. Restorative State

   The system is in a restorative state when there is a loss of load, and no constraint is violated. This situation occurs as a result of an emergency. The control objective in the restorative state is the safe transition from partial to 100 percent satisfaction of all customer demands in minimum time.

System security is employed to maintain the power supply satisfying customer demands which include security monitoring, security assessment, security control [48]. Security monitoring recognizes whether or not the system state is typically based on real–time system measurements. Further, security assessment refers to whether the normal state is secure or insecure regarding the set of postulated contingencies. In security control, emergency control is deployed in an emergency state, and restorative control is activated under load loss. System security control is classified into three categories as follows:

1. Preventive control

   Preventive control is mainly employed for an insecure state. An appropriate preventive action is used to make the system secure.

2. Emergency control

   In emergency control, corrective actions are applied to restore the system state being normal.

3. Restorative control

   The proper actions are constructed in restorative control to recover the service for all system loads.

The system security states and controls frameworks are described in Figure 2.1. The conventional approaches for power system security are depicted in Figure 2.2 which encompassed into three components namely monitoring, assessment and control.

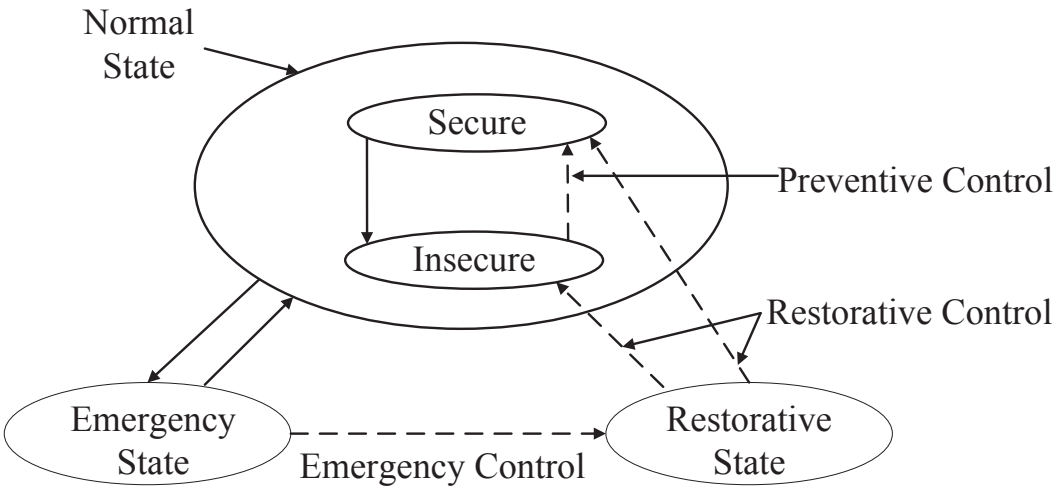

Figure 2.1. System security states and controls frameworks

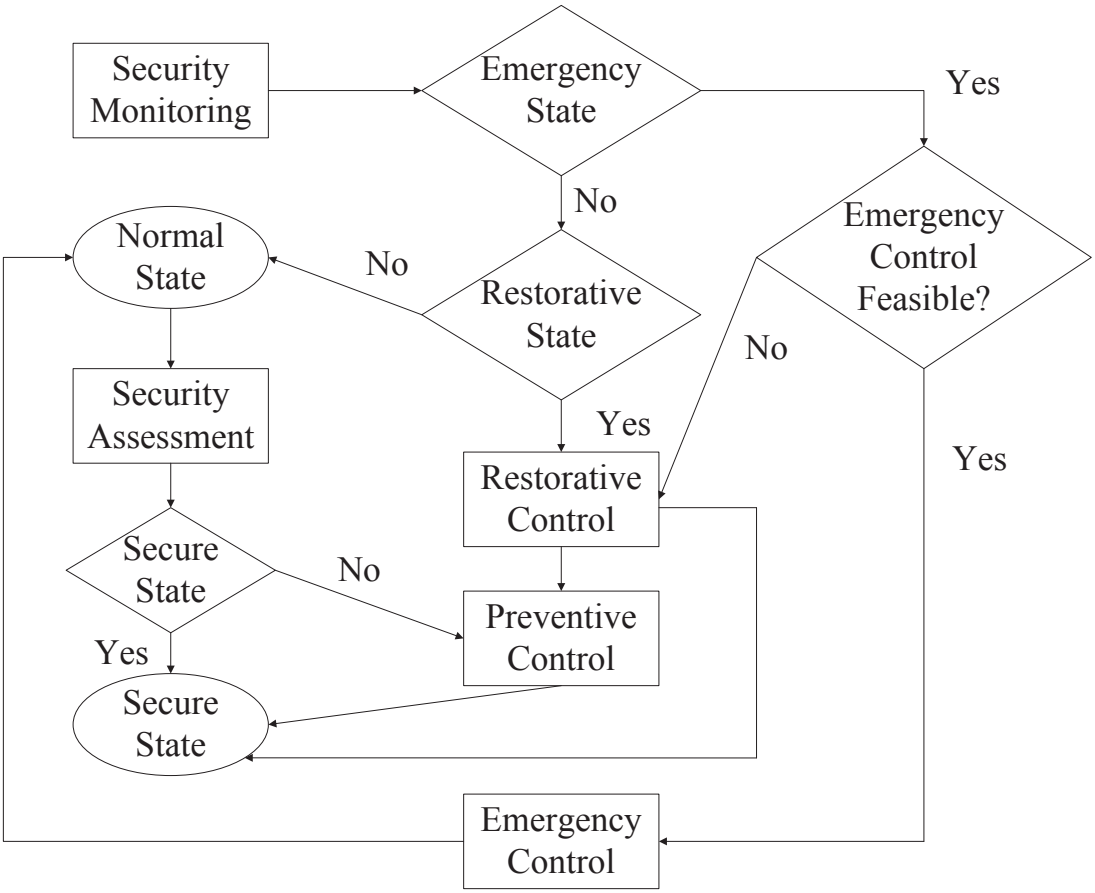

Figure 2.2. Conventional approaches for power system security

2.1.1. Reliability Criteria

Over the years, there is need to identify the scope of power system operation and to set the system reliability criteria. The description of reliability is provided in section

2.1. Commonly, the reliability of power system problems are defined theoretically and addressed in conditions of whether the prior reliability degree can be preserved, and what manner of problems may occur.

Reliability criteria of power system operation refer to the set of conditions which should be fulfilled in order to gain required reliability. Criteria are classified into two categories as follow [49]:

1. Index or variable is generally used for probabilistic criteria
   Indices present quantitative measures of reliability such as unsatisfied power supplies for annual desired energy or annual minutes of disruption of system load. One or more indices may be employed as criteria for power system operation and planning.
2. Attribute or performance test is specially designated for deterministic criteria.
   Attribute or performance test criteria refer to capable of power system operation withstand the set of contingencies. Attribute or performance test criteria present the definition of acceptable recovery for power system operation against the risk and severity of the contingencies.

These criteria have the difference for deterministic and probabilistic researches. The term "tests" are commonly used in relation to deterministic criteria where the power system operation may restrain a predetermined set of disturbances. While cut-off points of reliability indices are employed for probabilistic criteria [50, 51]. Two features include the probability (or frequency), and severity (or performance) of disturbances are easy to be recognized. These two features involve the elements of a probabilistic desired value, the expectation, of the severity. This expectation refers to “risk.” where it is used to assess reliability levels. When the events/disturbances with a higher frequency of occurrence have emerged, the power system operation with high performance is required to withstand those events/disturbances. The difficulty with deterministic criteria is that the criteria yield inconsistent decision making concerning risk. Low-risk cases are commonly included, and high-risk cases are neglected. The difficulty of probabilistic criteria determines the satisfaction of operators and planners.

In this thesis, reliability criteria in power system operation are defined as the ability of power generation units in order to preserve the supply of power to costumers in an acceptable standard which tolerance to contingency. The earliest and most easily calculated criterion namely deterministic criterion is specially employed to evaluate the

power system reliability in this thesis. Worldwide, the N-1 reliability standard under deterministic or defined attribute or performance test criterion is employed as a security criterion to evaluate power system operation. The application of this standard for evaluation of power system operation is to guarantee the supply of power in order to deliver electricity to all points of N electric power utilizations which should not be disturbed against any contingencies. In the case of deterministic criterion for power system operation, the power generation units are not degraded by any single contingency. Power flow equations before and after the contingency defined in the following form are useful for evaluation of N-1 security criterion.

$$\left.\begin{array}{l} \boldsymbol{f}^n(\boldsymbol{x},\boldsymbol{u},\boldsymbol{p})=0\,,\ \boldsymbol{g}^n(\boldsymbol{x},\boldsymbol{u},\boldsymbol{p})=0 \\ \boldsymbol{f}^n:\mathbb{R}^{B+G+L}\to\mathbb{R}^B,\ \underline{\boldsymbol{u}}\le\boldsymbol{u}\le\overline{\boldsymbol{u}}, \\ \boldsymbol{x}\in\mathbb{R}^B,\ \boldsymbol{u}\in\mathbb{R}^G,\ \boldsymbol{p}\in\mathbb{R}^L, n=0,1,\cdots,N \end{array}\right\} \tag{2.1}$$

The problem includes independent conditions with n=1~N, where n=0 implies pre-fault condition and n=1~N stands for N post-fault contingency conditions to present conventional N-1 security criterion. In system operation planning, while p is predicted, control u matching load p is determined to satisfy the constraints. Therefore, noted that (u, p) does not change before and after the fault when studying a static problem. Then, (u, p) is in common in (2.1), while different x may exist under each condition, where we describe x^0 to indicate pre-fault state and x^n, n=1~N, post-fault states. After all, the N-1 security criterion is satisfied with the following constraints for all x^0~x^N conditions.

(C1) Transmission line or transformer limit

$$g^{C1.n}(x^n,u,p)\le 0\ ,\ n=0,1,\cdots,N \tag{2.2}$$

(C2) Voltage limit

$$g^{C2.n}(x^n,u,p)\le 0\ ,\ n=0,1,\cdots,N \tag{2.3}$$

(C3) Voltage stability limit

$$g^{C3.n}(x^n,u,p)\le 0\ ,\ n=0,1,\cdots,N \tag{2.4}$$

(C4) Transient stability limit

$$g^{C4.n}(x^n,u,p)\le 0\ ,\ n=0,1,\cdots,N \tag{2.5}$$

(C5) Frequency deviation (power supply and demand control)

$$g^{C5.n}(x^n, u, p) \le 0 \ , \ n = 0,1,\cdots,N \tag{2.6}$$

where inequality constraints (2.2)-(2.6) can be composed of all factors over vector functions. Equations (2.2) and (2.3) express the constraints for transmission and voltage limit and can be solved by simple calculations. Equation (2.4) shows the restriction for voltage stability implying to calculate maximum load point. Equation (2.5) expresses the constraint for transient stability. Equation (2.6) represents the constraint for frequency deviation. By using mathematical expressions above, the objective of the power system operation and planning is to determine control variable u of generation output power to satisfy (2.1)-(2.6) with load p. In the following, the constraints (2.2)-(2.6) are summarized as follow:

$$\left.\begin{aligned} & g^n(x^n, u, p) \le 0 \qquad n = 0,1,\cdots,N \\ & g^n = [g^{C1.n}, g^{C2.n}, g^{C3.n}, g^{C4.n}, g^{C5.n}] \end{aligned}\right\} \tag{2.7}$$

where, $u_{\min} \le u \le u_{\max}$, x^n is the solution of $f^n(x, u, p) = 0$.

2.1.2. Power System Security Assessment

A power system security assessment is the process in power system operation that conducted in order to identify any violations in the power system operating state through monitoring power flows, voltages, and other power system operation components. Furthermore, another purpose of power system security assessment is especially for contingency analysis. In general, the elements of security assessment include system monitoring, contingency analysis, preventive and corrective actions.

The knowledge of the system states is necessary for security assessment of a power system. The first step may be conducted concerning power system security assessment is monitoring the system. System monitoring provides the up to date information on power system operation states to power system operators. This monitoring is carried out by measuring the behavior of voltage, power flows, generator output and other power system components which are sending to the control center by telemetry systems. The control center employs state estimator to process the data and calculates the best estimation of the system states. When the current operating state is known, the next task is the contingency analysis. Contingency analysis is carried out by preparing a list of

"credible" contingency cases. When contingencies occur, they must be detected immediately and evaluated regarding potential risk to the system. Evaluation the risks associated with each contingency, fast power flow solution approaches are employed. The selected contingencies are ranked in order based on their severity. The procedures carried out by power system operator to respond each unsafe contingency case are mostly in decreasing order of severity as follow:

a. System operation in a pre-contingency state is changed with a view to alleviate or remove the emergency which induced by contingency.
b. The control strategy is developed in order to mitigate the emergency.
c. When the emergency in post-contingency is very small, the power system operator is no need to take action.

In the conventional approach, contingency analysis is carried out by simulating each contingency using the base-case model of a power system. The investigation for a post-contingency operating state is employed to identify the violations in regarding power system operating limit. The main point of this part is power flow solution must be simulated for each contingency event. However, several difficulties in the following conditions may face in practical studies [7]:

1. Develop a suitable power system model. This model depends on the representation and accuracy of post-contingency state.
2. Specify the contingency cases that must be considered.
3. Large consuming time is required in order to solve power flow calculation for a large number of contingency cases.

The primary components of contingency analysis include contingency definition, selection, and evaluation. Contingency definition is the function that requires minimum consuming time compared to other approaches. The contingency cases which prospect of occurrence is adequately high are selected in contingency list to be processed in the Energy Management System (EMS). Contingency selection is unique process offering a great computational saving which has purposed to reduce the long list of contingencies by removing a vast majority of cases having no violations. The contingency cases are ranked in order of their severity. Contingency evaluation using ac/dc power flow is then carried out on the successive individual cases in alleviating order of severity. The process is iterative until reach a specified time, or a maximum number of cases has been covered. Contingency selection and evaluation are incorporated into one process for some cases. Preventive and corrective actions are used to preserve a feasible and secure power system

operation or to recover the power system operating states caused by the disturbance to a safe operating state. Altering transformer taps and phase shifters, switching of VAR compensating devices are the example of corrective actions which are mainly automatic in nature, and normally in short duration. While preventive actions such as generation rescheduling involve longer time scales. Security-constrained optimal power flow is an example of rescheduling the generations in the system in order to ensure a secure operation.

2.2. Robust Power System Security

As described in section 2.1, power system security relates to the ability of power system to determine whether, and to what extent, a power system reasonably safe from severe interference to its operation. These days, the problems of power system security acquire more attention from many researchers where deterministic and probabilistic approaches solve those issues. The idea concerning conventional N-1 security criterion has been proposed in [1], [2], [5], [7], [10] and is employed in various power system studies. A new criterion defined as the extension of conventional N-1 security criterion which satisfies all predetermined constraints under the disturbed condition as shown in Figure 2.3 is described in this section. This criterion is called robust power system security. This new criterion has the same concept with the conventional method, while the differences are the approach to treat uncertainties. Robust power system security region implies the area of power system operating states in secure condition under uncertainties caused by load and renewable energy (RE) predictions errors.

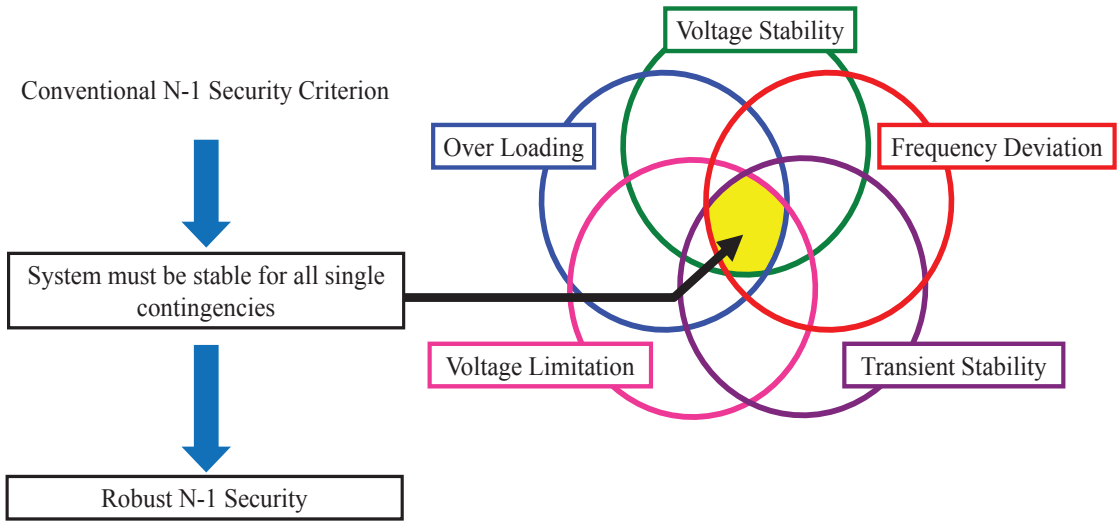

Figure 2.3. The definition of robust power system security [52]

2.2.1. Concept of Robust Power System Security

The concept of robust power system security is depicted in Figure 2.4. Each type of security region in Figure 2.4 is defined in the space for control vector u, generation output power at t_1 and t_2.

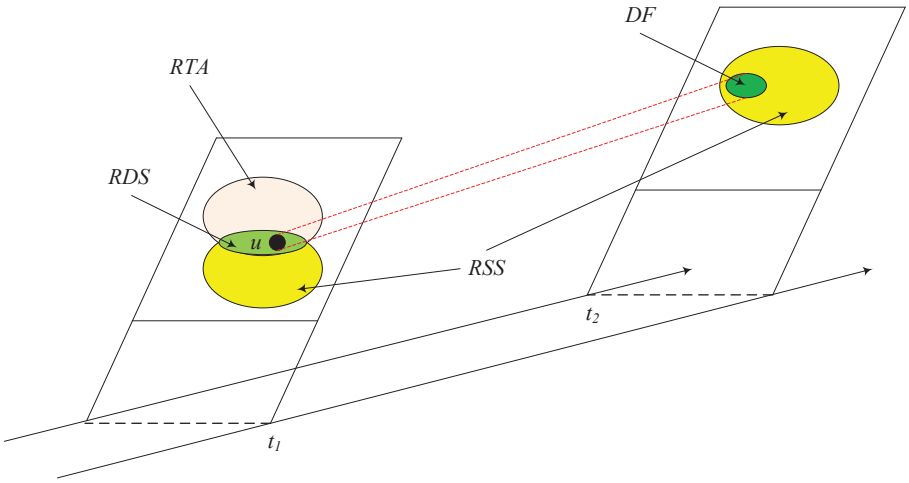

Figure 2.4. The general concept of robust power system security [55]

Security regions are decomposed as follow: Static Security (SS) region, Robust Static Security (RSS) region, Dynamic Feasible (DF) region, Robust Dynamic Feasible (RDF) region, Robust Reachable Region for Time-Ahead (RTA) security and Robust Dynamic Security (RDS) region.

Robust power system security is originally proposed at the first time by Prof. Naoto Yorino et all in [53, 54]. In this study, the authors propose the concept of "Robust Security (RS)" and the "RS region" in order to evaluate power system security against uncertainties. The more amount of PV being integrated into power system grid, the more security area shrinks. IEEJ WEST10 model is used to examine the proposed approach. The performance of proposed method is examined by two cases with different level of uncertainty associated with PV output, where transient stability case study is included. Hereafter, the concept of robust power system security (RS) is applied to evaluate N-1 security quantitatively [34]. Three machine power system models are employed to demonstrate the robustness of proposed method. A new assessment index based on robust dynamic security (RDS) is utilized for quantitative analysis. Time window approach is applied in order to compute the fluctuation of PV output where any time window intervals

are calculated by using sun's energy data from Hiroshima Meteorological Observatory. In summarization, three satisfactory primary results are obtained as follow:

1. The correlation of PV integration regarding N-1 security yields an apparent trade-off.
2. When PV generation unit installed in power system grid is raised, the area of RDS region tends to shrink. The security region satisfying N-1 security criterion disappears as the impact of high penetration of PV to power system network.
3. The region fulfilling N-1 security criterion is effectively improved by installing battery storage.

   Battery storage is incorporated in power system grid to enlarge the robust dynamic security (RDS) security region. Therefore, the security region for ensuring the N-1 security criterion becomes larger.
4. Visualization of the security region is performed in order to the power system operator easily pay attention the N-1 security circumstances.

   Graph visualization to represent the robust power system security region is actually serviceable for power system operator due to each security region is observable, and power system operation condition is easily recognized.

In [35], the concept of robust security is performed for dynamic economic load dispatch (DELD) problem. In this study, periodic evaluation of generation schedule plays a key role in updating robust security region against forecast error and defines a credible and rigorous power system operation response to incidental changes in supply output. Six-bus power system model is used to examine the robustness of proposed method for DELD which the security limit for transmission line flow is treated. IEEJ West Japan 10-machine system is applied to investigated transient stability problem from the viewpoint of the robust security issue.

In this thesis, a new mathematical model is proposed in order to obtain the bounds of security region. The difference between the bounds represents the diameter of security region, which can be employed as a security measure. This formulation and method are applied to calculate the size of security region for robust static security (RSS) and robust dynamic feasible (RDF) security problems, respectively.

In robust power system security, satisfying N-1 security criterion for given load p is equivalent to obtaining the feasible region of control variable u within security region for all contingencies. That is,

$$\left.\begin{aligned} &SS_u(p)=\left\{u \mid SS_u^0(p) \bigcap SS_u^1(p) \bigcap \cdots \bigcap SS_u^N(p)\right\} \\ &SS_u^n(p)=\left\{u \mid \underline{u} \le u \le \bar{u},\ f^n=0,\ g^n \le 0\right\} \\ &n=0,1,\cdots,N \end{aligned}\right\} \tag{2.8}$$

The security region defined in above is called "Static Security (SS) region" which refers to a snapshot of power system operation at a particular time. SS region is defined as the area of generation unit output to withstand under specific parameter values of p within N-1 security criterion. In other words, a power system operating point within SS region is equivalent to that the power system states are operating in secure condition satisfying N-1 security criterion.

In order to compute the size of static security (SS) region, the hyper-plane described in (2.9) with a pre-specified normal vector c is employed [55]

$$c^T u = \alpha \tag{2.9}$$

The upper and lower of SS region bounds are delineated as follow [55].

$$\underline{\alpha}_{SS(p)} \le \alpha \le \bar{\alpha}_{SS(p)} \tag{2.10}$$

The upper and lower limits of SS region matching N-1 security criterion is computed using formulation in (2.11) and (2.12), respectively [55].

$$\bar{\alpha}_{SS(p)} =: \max_u \ c^T u \tag{2.11}$$

$$\underline{\alpha}_{SS(p)} =: \min_u \ c^T u \tag{2.12}$$

The upper and lower bounds of SS region in (2.11) and (2.12) must satisfy within (2.2)-(2.6). The problems (2.11) and (2.12) are easily solved using well-known optimization approach. The diameter *d* of the SS bounds is employed as security index for the direction of vector *c* [55].

$$d = \frac{1}{\| c \|}(\bar{\alpha}_{SS} - \underline{\alpha}_{SS}) \tag{2.13}$$

In dynamic power system operation, generator output is restricted by its dynamic operation constraint where defined by output power change limitation or ramp-rate constraint due to thermal stress. Unit commitment and reactive power control problems are with such constraints. The controllable generator outputs at the two-time point from $u(t_1)$ to $u(t_2)$ which bounded by a constraint as a function of control duration. In this study,

t_1 implies the current time or initial time point, and t_2 represents future time points.

$$h(u(t_1), u(t_2), \delta t) \leq 0 \tag{2.14}$$

The state (x_1, u_1, p_1) at t_1 is assumed as an initial operating point, and p_2 at $t_2 = t_1 + \delta_t$ is provided as for future time point. Thus, the future time point (x_2, u_2, p_2) at t_2 is obtained satisfying power flow equation and dynamic operation constraint (2.14). This region is called Dynamic Feasible (DF) region. DF region refers to the area in which the usage of generators attains up to their maximum capacity from u_1 of generator output at t_1 to u_1 at t_2 based on load prediction p_2. DF region takes into account the dynamic constraints and the power flow equations and does not duly consider security constraints, interpreting the minimum constraints for power system operation. A sequential computation approach of DF is provided in [34, 53]. The DF region is defined as follows,

$$DF_{u2}(u_1, p) = \left\{ u_2 \mid h(u_1, u_2, \delta t, p_1, p_2) \leq 0,\ f^0(x_2, u_2, p_2) = 0 \right\} \tag{2.15}$$

2.2.2. Robust Static Security (RSS)

In conventional power system operation and planning, an electrical load of p is easily predicted since it is almost patterned and the uncertainty of load prediction is small or very unlikely. However, high integration of renewable energy (RE) in power system network is essential to be observed and analyzed due to the fluctuation of RE outputs are influenced by weather condition. These conditions cause large error prediction of RE outputs and the uncertainties of RE outputs should be taken into account in power system operation and planning.

Uncertainties are introduced in parameter vector p in order to evaluate the power system security region. The parameter values of p with uncertainties are given as follow.

$$R_P = \{ p \mid \underline{p} \leq p \leq \overline{p} \} \tag{2.16}$$

When uncertainties are incorporated in parameter p in (2.16), the region of generator unit output matching the N-1 security standard exists inside the intersection of static security (SS) region in (2.8). Robust static security (RSS) region implies the region inside control variable u satisfying N-1 for all possible parameter variations as follows.

$$RSS_u = \left\{ u \mid u \in \bigcap_{p \in R_p} SS_u(p) \right\} \tag{2.17}$$

The bounds of RSS region are defined as follow [55].

$$\underline{\alpha}_{RSS} \le \alpha \le \bar{\alpha}_{RSS} \tag{2.18}$$

The upper bound of RSS region $\bar{\alpha}_{RSS}$ associates with the lower bound of $\bar{\alpha}_{SS(p)}$ for all probable values of p. The following formula is proposed to obtain the upper and lower bounds satisfying the N-1 security criterion.

The maximum limit of RSS region.

$$\bar{\alpha}_{RSS} = \min_{p \in Rp} \bar{\alpha}_{SS(p)} \tag{2.19}$$

The equation (2.19) can be presented as in (2.20).

$$\bar{\alpha}_{RSS} =: \min_{p \in Rp} \{\max_{u} c^T u\} \tag{2.20}$$

The minimum limit of RSS region.

$$\underline{\alpha}_{RSS} = \max_{p \in Rp} \underline{\alpha}_{SS(p)}$$

The problem (2.20) is re-written as follows.

$$\underline{\alpha}_{RSS} =: \max_{p \in Rp} \{\min_{u} c^T u\} \tag{2.21}$$

The RSS problems (2.20) and (2.21) are defined as a min-max optimization problem. The bounds of RSS region (2.25) and (2.26) are subjected to (2.2)-(2.6). The appropriate techniques are developed in order to solve the complexity of this problem which described in the Chapters 3 and 4.

The security indicator d to compute the distance between upper and lower bounds of RSS region is calculated in the same manner in (2.13).

2.2.3. Robust Dynamic Feasible (RDF)

The estimation of fluctuation parameter such as load as well as renewable energy (RE) forecast in short or long term period is required and considered in power system operation and planning. When $p(t)$ is assumed as fluctuation parameter at time t, the estimation model is defined in the following form.

$$p(t) = \hat{p}(t \mid t - \delta t) + \Delta(\delta t)$$

$$\Pr\left\{\underline{\Delta}(\delta t) \le \Delta(\delta t) \le \overline{\Delta}(\delta t)\right\} = CL,\ 0 \le CL \le 1 \tag{2.22}$$

where, $\hat{p}(t \mid t-\delta t)$ is the forecast of $p(t)$ at t - δt, and $\Delta(t \mid t-\delta t)$ is the prediction error. The error is noticed as "uncertainty", which can not be obviated and rises concerning forecast time δt. The confidence interval (CI) is employed to represent the uncertainty where upper and lower bounds are characterized by confidence level, CL. The confidence interval of *p(t)* at time *t* is defined as follows.

$$R_p = \{p \mid \hat{p} + \underline{\Delta} \le p \le \hat{p} + \overline{\Delta}\} \tag{2.23}$$

The expression permits uncertainty Δ around prediction $\hat{p}$ for a particular value of *CL*. The bounds of uncertainties Δ are regarded as maximum forecast error in *p*. The definition of robust dynamic feasible (RDF) region is provided as follows.

$$RDF_{u_2(u_1)} = \left\{u_2 \mid u_2 \in \bigcap_{p_1 \in R_{p1}, p_2 \in R_{p2}} DF(u_1, p)\right\} \tag{2.24}$$

The formulation to obtain upper and lower bounds of RDF security region is extended from RSS region case problem. The problem formulation of RDF security region utilizes the interval time points $t = 1, 2, ...$where t_1 is referred as an initial operating point. The size of RDF security region is defined in the following form.

The upper and lower limits of RDF security region [56, 57, 58] are provided as follow.

$$\overline{\alpha}_{RDF}(t) =: \min_{p \in Rp} \{\max_{u} c^T u(t)\} \tag{2.25}$$

$$\underline{\alpha}_{RDF}(t) =: \max_{p \in Rp} \{\min_{u} c^T u(t)\} \tag{2.26}$$

The RDF security region problems (2.25) and (2.26) are subjected to (2.2)-(2.6) and (2.14). The solution of RDF security problems (2.25) and (2.26) is obtained based on time point series $t = 2, 3, \ldots$. The initial operating point is determined by power system operators in order to evaluate the security region at each time point for power system operation. Security index *d* is calculated in the same way as in (2.13) to assess the reliability of the power system operation.

Further, the definitions of a robust reachable region for time-ahead (RTA) security and robust dynamic security (RDS) in details are provided in [34], [35], [53].

CHAPTER 3 : EVALUATION OF ROBUST STATIC SECURITY (RSS) REGION UNDER UNCERTAINTIES

3.1. Introduction

This chapter describes the application of a new approach for evaluating robust static security (RSS) problem against uncertainties, where the concept of RSS in detail was described in chapter 2. The RSS problem formulations are composed in deterministic and linear constraints approaches and solved by linear programming (LP) method. A small power system model is used to examine the proposed method with three case studies. Case 1 implies that the PV outputs are accurately forecasted. Case 2 stands for a typical case with 20% of prediction errors of PV outputs are examined. Case 2D implies Case 2 with strict transmission line limits. Case 3 represents a severe uncertain case in which the errors in PV output forecast are considerably increased.

3.2. Power System Model for Robust Static Security (RSS)

The problem formulation to calculate RSS region is presented in this section. All stability factors on the power system network are considered in evaluating the RSS area. The well-known constraints for static load dispatch problem are used in this study as follow.

$$e^T \cdot (u + p) = 0 \tag{3.1}$$

$$\underline{P}_{TL} \le S^{(n)} \cdot (u + p) \le \overline{P}_{TL} \qquad n = 1 \ldots N \tag{3.2}$$

$$\underline{u} \le u \le \overline{u} \tag{3.3}$$

$$R_P = \{p \mid \underline{p} \le p \le \overline{p}\} \tag{3.4}$$

$$\underline{p} = \underline{P}_R - \overline{P}_L, \overline{p} = \overline{P}_R - \underline{P}_L \tag{3.5}$$

where, e=[1 1..1]^T, $\overline{P}_{TL}, \underline{P}_{TL}$: upper and lower limits of transmission line flows, $S^{(n)}$: transformation matrix from node injection to line flow for fault n (DC power flow), n: fault number (n = 0 for normal condition), N : Contingency conditions, $\overline{u}, \underline{u}$: upper and lower limits of controllable parameter u, $\overline{p}, \underline{p}$: upper and lower of Confidence

Interval (CI) for uncontrollable variable p, $\overline{P}_R, \underline{P}_R$: CI of renewable energy (RE), $\overline{P}_L, \underline{P}_L$: CI of electricity load demands. Equation (3.1) implies the demand and supply (DS) balance constraints while the transmission lime limits are represented by (3.2).

3.3. Formulation of Static Security (SS) Region

The parameters in power system used in this thesis include controllable parameter P_G and uncertain parameters P_R and P_L as follow.

$$u = P_G \tag{3.6}$$

$$p = P_R - P_L \tag{3.7}$$

The feasible region within the set of constraints (3.1)-(3.5) for uncertain parameter p is defined as a static security (SS) area which is described as $SS_u(p)$ in the following form.

$$SS_u^{(n)}(p) = \left\{ u \mid e^T \cdot (u+p) = 0,\ \underline{P}_{TL} \le S^{(n)} \cdot (u+p) \le \overline{P}_{TL}, \underline{u} \le u \le \overline{u} \right\} \tag{3.8}$$

Then, static security region is defined as the intersection of feasible areas for all contingencies based on (3.8).

$$SS_u(p) = \left\{ u \mid SS_u^{(0)}(p) \cap SS_u^{(1)}(p) \cap \cdots \cap SS_u^{(N)}(p) \right\} \tag{3.9}$$

3.4. Measure of Static Security (SS) Region Size

The hyper-plane in (3.10) with a pre-specified normal vector c is employed in order to measure the size of static security region [55].

$$c^T u = \alpha \tag{3.10}$$

When parameter α varies on its movement, there is exit intersection of the static security region and hyper-plane if static security region exists. The region of "α" is represented as follows [55].

$$\underline{\alpha}_{SS(p)} \le \alpha \le \overline{\alpha}_{SS(p)} \tag{3.11}$$

The concept of static security (SS) region is described in Figure 3.1. Then, the upper and lower bounds of static security area are proposed in (3.12) and (3.13).

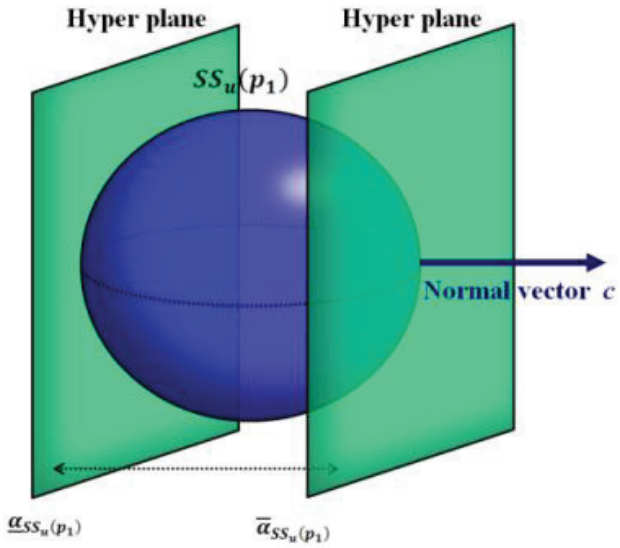

Figure 3.1. Measure of static security region size using hyper-planes [55]

When the hyper-plane α is maximized, the upper limit of static security region is obtained. In vice versa, the lower limit of static security region is gained by minimizing the hyper-plane α. The sphere depicted in Figure 3.1 is the static security region satisfying the set of constraints (3.1)-(3.4). Thus, the size of static security area is known by the index alfa and its upper and lower bounds.

Upper bound (UB) of static security (SS) region:

$$\overline{\alpha}_{SS(p)} =: \max_{u} \; c^T u \tag{3.12}$$

Subject to (3.1)-(3.4) under given p.

Lower bound (LB) of static security (SS) region:

$$\underline{\alpha}_{SS(p)} =: \min_{u} \; c^T u \tag{3.13}$$

Subject to (3.1)-(3.4)) with provided p.

The problems (3.12) and (3.13) can be solved by optimization technique such as linear programming method.

3.5. Region Size Problem for Robust Static Security (RSS)

Referring to Chapter 3, robust static security (RSS) region is defined as the intersection for the variation of $SS_u(p)$ movements. When the renewable energy (RE) output such as PV is accurately forecasted, the size of robust static security region is maximum. In other hands, robust static security area shrinks as CI in parameter p is

extended. The computation of upper and lower limit of α for the robust static security region is expressed as follow [55].

$$\underline{\alpha}_{RSS} \le \alpha \le \overline{\alpha}_{RSS} \tag{3.14}$$

To calculate the size of robust static security (RSS) region, $\overline{\alpha}_{RSS}$ corresponds to the lower bound of $\overline{\alpha}_{SS(p)}$ for all possible parameter values of p in CI. Thus, it can be represented as the following condition.

Upper bound (UB) for robust static security (RSS) region:

$$\overline{\alpha}_{RSS} = \min_{p \in Rp} \overline{\alpha}_{SS(p)} \tag{3.15}$$

The problem (3.15) is re-written as min-max optimization model in the following form.

$$\overline{\alpha}_{RSS} =: \min_{p \in Rp} \{\max_{u} c^T u\} \tag{3.16}$$

Subject to (3.1)-(3.4)

Lower bound (LB) for robust static security (RSS) region:

$$\underline{\alpha}_{RSS} = \max_{p \in Rp} \underline{\alpha}_{SS(p)} \tag{3.17}$$

The equation (3.17) is represented in min-max optimization framework as follows.

$$\underline{\alpha}_{RSS} =: \max_{p \in Rp} \{\min_{u} c^T u\} \tag{3.18}$$

Subject to (3.1)-(3.4).

Figure 3.2 shows the deviation of the upper and the lower bounds of static security region when p is varied, in which the lowest upper bound and the highest lower bound define the bounds of robust static security region concerning normal direction c.

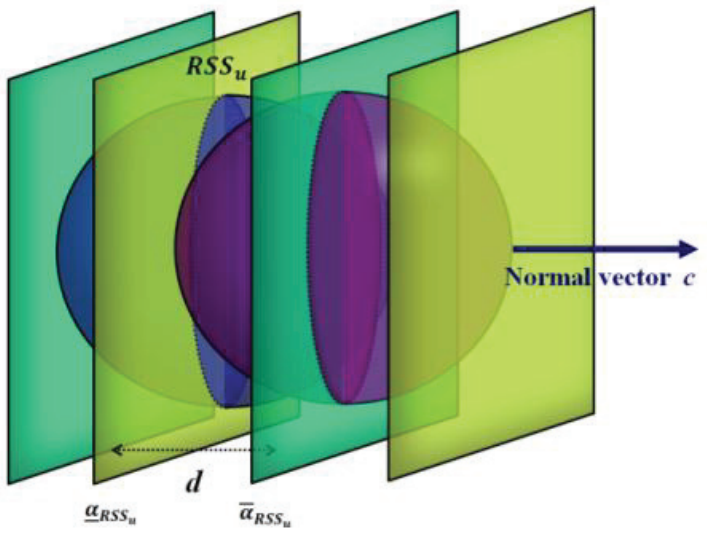

Figure 3.2. Measure of robust static security size for deviations of static security region [55]

In this case, the worst minimum $\underline{\alpha}_{RSS}$ is the maximum of the lower bound $\bar{\alpha}_{SS(p)}$. The worst maximum $\bar{\alpha}_{RSS}$ is the minimum of the upper bound $\bar{\alpha}_{SS(p)}$. The distance d between the bounds is a useful index to present the robust static security region size for the direction of vector c.

$$d = \frac{1}{\| c \|}(\bar{\alpha}_{RSS} - \underline{\alpha}_{RSS}) \tag{3.19}$$

Security index d is positive when robust static security (RSS) is existence, and its absolute value expresses the region size, while the negative value of d shows that robust static security is nonexistence. The larger the security index, the system is more easily controlled within the region where the system security is maintained. When the different direction of c is set, the length of robust static security in different direction c can be obtained. Since d represents the length of the intersection, when the volume of the intersection depicted in Figure 3.2 becomes small, d always becomes small except the situation where an exceptional direction is selected. When the volume of the intersection disappears, d always becomes negative without exception.

The problems (3.16) and (3.17) are the new type of problem to be required in the power system operation when the uncertainty is increased. At present, even though the linear problem studied here is not solved by the conventional linear programming (LP) approach, the proposed problem can be solved efficiently in the future based on a particular technique.

3.6. Approximate Solution of Region Size Problem for Robust Static Security

In this section, a solution method for the problems of (3.16) and (3.17) is provided. First, $\tilde{c}$ is introduced which satisfies (3.20) [55].

$$e = c + \tilde{c} \tag{3.20}$$

The elements of c and $\tilde{c}$ consist of either 0 or 1. Regarding the expression (3.20), demand-supply (DS) constraint (3.1) is re-written as follows.

$$c^T u + \tilde{c}^T u + e^T p = 0 \tag{3.21}$$

or

$$\sum_{i \in C} u_i + \sum_{j \notin C} u_j + \sum_k p_k = 0 \tag{3.22}$$

The first term corresponds to the objective of (3.16) and (3.17), the sum of the outputs of the selected controllable generators specified by vector c; C is the set of indices i of the selected generators. The second term is the sum of the other generator outputs, which is in this thesis referred as "slack generators." The third term is the sum of loads and RE generations including uncertainties. It is generally stated that, given the third term, the objective is maximized when the second slack term is minimized to meet DS balance (3.1) or (3.22). Furthermore, the maximized objective is most bounded when the third term appears as its maximum. Basically, this is the solution to the problem (3.16), where additional line flow limits may further constrain the solution. This characteristic is due to (3.1). The following example may suggest a practical solution. A two-bus system used in this example is shown in Figure 3.3.

[Example] $u = [u_1\ u_2]^T$, $u = [p_1\ -50]^T$, $c = [1\ 0]^T$, $\tilde{c} = [0\ 1]^T$

$$\bar{\alpha}_{RSS} = \min_{p \in Rp} \{\max_u c^T u\} = \min_{p \in Rp} \{\max_{u_1} u_1\} \tag{3.23}$$

Subject to

(3.1): $u_1 + u_2 + p_1 = 0$

(3.2): $-30 \le (u_1 + p_1) - (u_1 + p_1) \le 30$

(3.3): $5 \le u_1 \le 30,\ 10 \le u_2 \le 30\,;\ 0 \le p_1 \le 20 = \overline{p}_1$

Solution without (3.3) : $u_1^* = 20,\ u_2^* = 10,\ p_1^* = 20$

Solution : $u_1^* = 10,\ u_2^* = 20,\ p_1^* = 20$

The observation of the example shows that the solution is obtained at $p_1 = \overline{p}_1$ and that the larger objective is obtained for the less constrained case without (3.2). This is the case even if uncertainty in p_2 is existence. Another issue to be examined is the feasibility of the problem. In this example, when uncertainty is extended as $\overline{p}_1 = 40$, there are no solutions for $25 < p_1 < 40$.

Based on the above investigation, an approximate solution for the following problem is provided.

$$\overline{\alpha}_{RSS} = \min_{p \in Rp} \{\max_{u} c^T u\} = \min_{p \in Rp} \max_{u} \left\{-\tilde{c}^T u - e^T p\right\} \tag{3.24}$$

Subject to (4.1)-(4.4) .

(Step U1): Feasibility check.

Perform the following minimization.

$$\min_{p \in Rp} \left\{-e^T p\right\} \ \Leftrightarrow\ \max_{p \in Rp} \left\{e^T p\right\} \tag{3.25}$$

Subject to (4.1)-(4.4)

The solution of (3.25) is expressed as p^*. If $p^* = \overline{p}$, the problem is regarded as feasible, where u is a dependent variable and is successfully controlled to maximize the objective to the possible boundary.

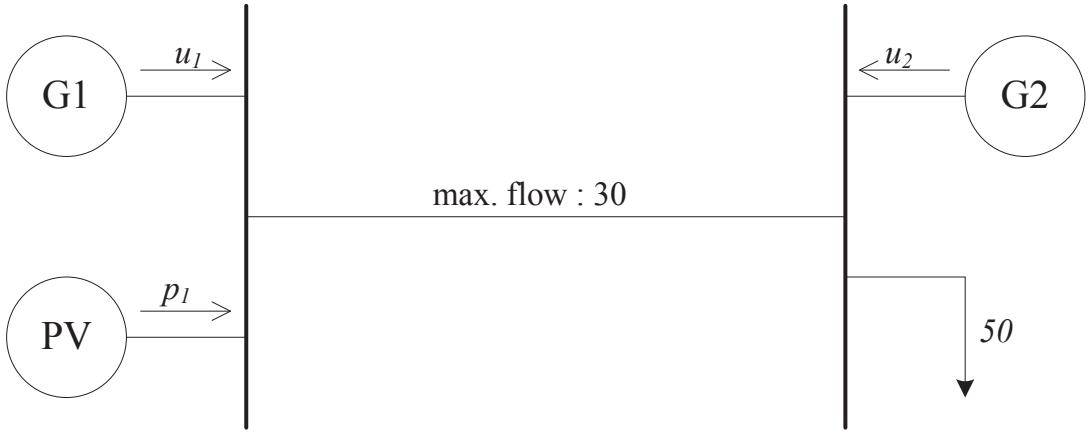

Figure 3.3. A two-bus system

Otherwise, the problem is infeasible, implying that u is nonexistence for $p^* < p < \bar{p}$ satisfying (3.1)-(3.4). In this case, the cause of the infeasibility and prepare a countermeasure should be identified. Noted that the importance of the constraints differs. After checking feasibility, the following problem is solved.

(Step U2): Solve the following problem with $p = \bar{p}$.

$$\bar{\alpha}_{RSS} = \max_{u} c^T u \tag{3.26}$$

Subject to (3.1)-(3.4)

Noted that the solution of (3.26) is not necessarily the optimal solution of the original problem of (3.16) since $p = \bar{p}$ does not provide the exact binding point of the line flow constraint of (3.2). In general, line flow limit (3.2) is less important since its violation for a short period may be permitted in actual power system operation. Nevertheless, the obtained solution satisfies all the constraints including (3.2) and therefore, provides a slightly relaxed value of the objective, which is practically useful. The obtained solution precisely captures DS balance (3.1), which is critically important to avoid the system collapse.

In the same way, the following procedure is suggested for the lower bound $\underline{\alpha}_{RSS}$.

(Step L1): Feasibility check.

$$\max_{p \in Rp} \left\{ -e^T p \right\} \quad \Leftrightarrow \quad \min_{p \in Rp} \left\{ e^T p \right\} \tag{3.26}$$

Subject to (3.1)-(3.4).

(Step L2): Solve the following problem with $p = \underline{p}$.

$$\underline{\alpha}_{RSS} = \min_{u} \; c^T u \tag{3.27}$$

Subject to (3.1)-(3.4).

Noted that Step U1 or L1 may be omitted when the feasibility check is unnecessary.

3.7. Numerical Studies

The RSS region size is examined by the proposed method using a small-scale power system in Figure 3.4. A line fault at point A is assumed as a contingency, where one of the double circuit lines is opened. The system model consists of 3-thermal generators and 3-PV generation resources.

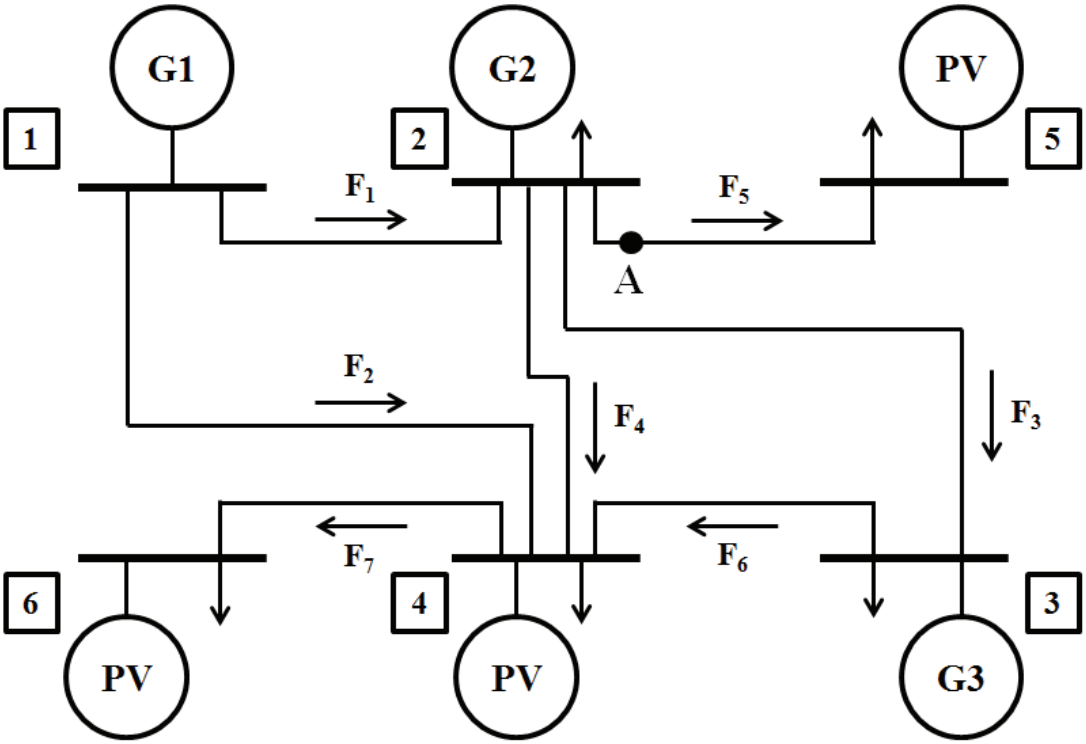

Figure 3.4. A small-scale power system

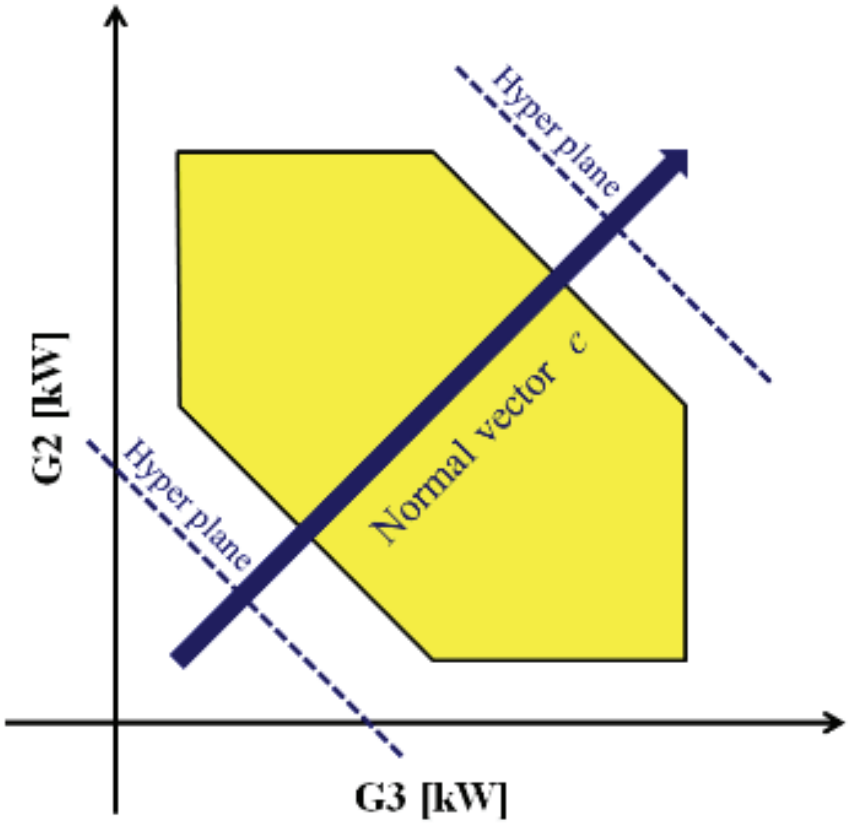

Figure 3.5. Placement of RSS, hyperplane and normal vector

The amount of PV generation is considered 30% of the total load. Tables 3.1 and 3.2 show the upper/lower limit of generator output, load and PV capacities for individual nodes with the elements of vector c for the RSS size evaluation. Transmission line limits are listed in Table 3.3. However, $\pm$ 1200kW is mainly used for all transmission line limits for Case 2D.

The problem is solved by the proposed method in which normal vector c = [0 1 1 0 0 0]^T is selected to measure RSS. The setting of c indicates the system capability focusing on the behavior of generators G_2 and G_3. The placement of RSS region, the hyper-plane with normal vector c, and upper/lower limits ($\underline{\alpha}_{RSS}$,$\bar{\alpha}_{RSS}$) of RSS for the direction c in the G_2-G_3 output plane are depicted in Figure 3.5.

Table 3.1. Generator's upper/lower limits [kW]

	G_1	G_2	G_3	Total
Lower limit	1000	630	1130	2760
Upper limit	2000	1250	2250	5500

Table 3.2. Load consumptions, PV capacities, and normal vector c

	Node 1	Node 2	Node 3	Node 4	Node 5	Node 6	Total
Load [kW]	0	500	500	2000	1000	1000	5000
PV [kW]	0	0	0	500	500	500	1500
c	0	1	1	0	0	0	

Table 3.3. Transmission line limits [kW] for Cases 1, 2, and 3

	Line 1	Line 2	Line 3	Line 4	Line 5	Line 6	Line 7
Lower limit	-1600	-1200	-1600	-2000	-1400	-1800	-1200
Upper limit	1600	1200	1600	2000	1400	1800	1200

Table 3.4. Uncertainty setting of CIs for PV output power [kW]

Case	PV_1		PV_2		PV_3	
	Lower	Upper	Lower	Upper	Lower	Upper
1	250	250	250	250	250	250
2、2D	200	300	200	300	200	300
3	50	450	50	450	50	450

Table 3.5. Solution of RSS region limits $\underline{\alpha}_{RSS}$,$\bar{\alpha}_{RSS}$ and indicator d

		G_1 [kW]	G_2 [kW]	G_3 [kW]	α	d	Area
Case 1	Lower limit	2000	805	1445	2250	707	543100
	Upper limit	1000	1146	2104	3250		
Case 2	Lower limit	2000	807	1592	2400	494	409800
	Upper limit	1000	1144	1956	3100		
Case 2D	Lower limit	2000 2000	1176 1178	1224 1222	2400 2400	259 174	30800
	Upper limit	1337 1753	1250 1250	1516 1396	2766 2647		
Case 3	Lower limit	2000	729	2121	2850	-141	0
	Upper limit	1000	1153	1496	2650		

Three cases of uncertainty settings are assumed in Table 3.4, where upper and lower limits of PV output forecast are indicated by CIs. Case 1 represents no uncertainty case where PV outputs are accurately predicted. Case 2 stands for a typical case where 20% of forecast errors are assumed in the setting of CI for PV outputs. Case 2D implies Case 2 with strict transmission line limits and stands for the case where the exact solution can not be obtained, but the sufficiently approximate solution is provided by the proposed method. Case 3 represents a severe uncertain case in which the errors in PV output forecast are considerably increased with a large setting of CIs, assuming a sudden change in the weather.

Table 3.5 shows the solutions of the proposed maximization and minimization problems for the measurement of RSS region, which includes the output powers of generators, limits, and indicator d. Figure 3.6(a), 3.6(b), 3.6(c) and 3.6(d) show RSS regions respectively for Cases 1, 2, 2D and 3 in the G_2-G_3 output plane.

The obtained solution points in each case are marked by “triangular points” which are located on the border of RSS. An exhaustive search method is used to obtain the exact solution. The result was that they agree to each other for cases 1, 2 and 3 but the slight error was observed in case 2D. The gross area of RSS region [GW^2] is also computed based on the exhaustive search method and listed for each case in Table 3.5.

From the simulation results, the following conditions are observed: In no uncertain case 1, the region of RSS is large enough confirmed by the value of d = 707 in Table 3.5, as is also seen in Figure 3.6(a), where system security may be easily achieved. In case 2 with 20% uncertainty in PV outputs, RSS shrinks as seen in Figure 3.6(b) with d = 494, where it becomes more difficult to dispatch generator outputs in the security region, RSS. Careful system operation is required to preserve system security by fully using the available system capability. In case 2D where more severe line flow limits are imposed, less value of d is computed.

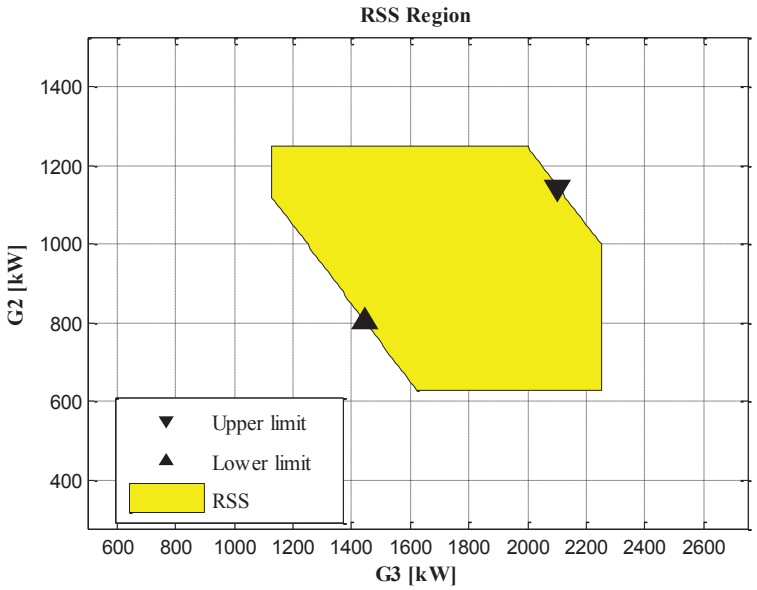

(a) Case 1

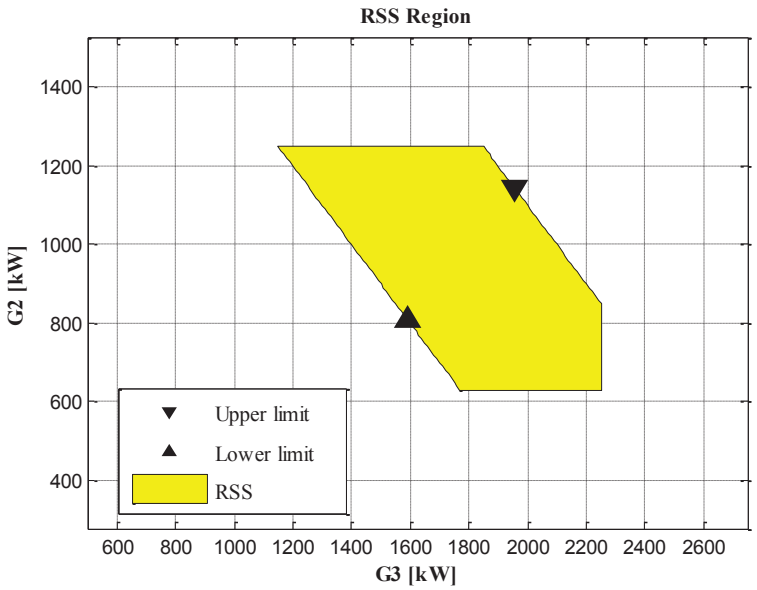

(b) Case 2

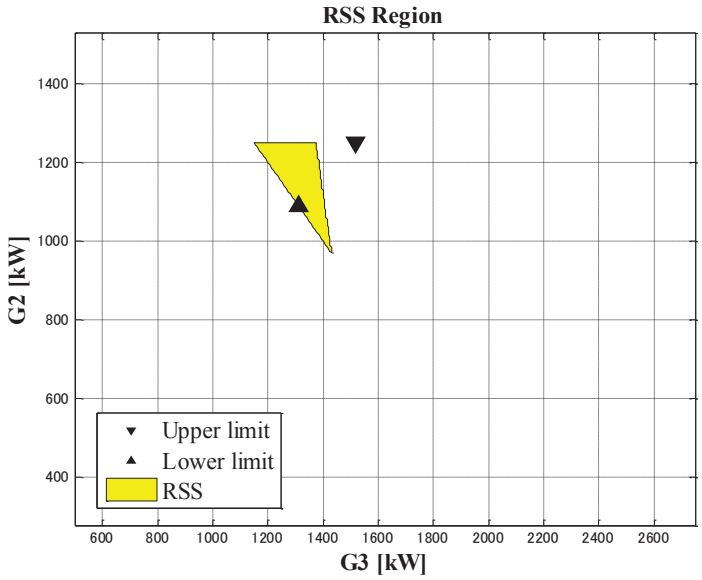

(c) Case 2D

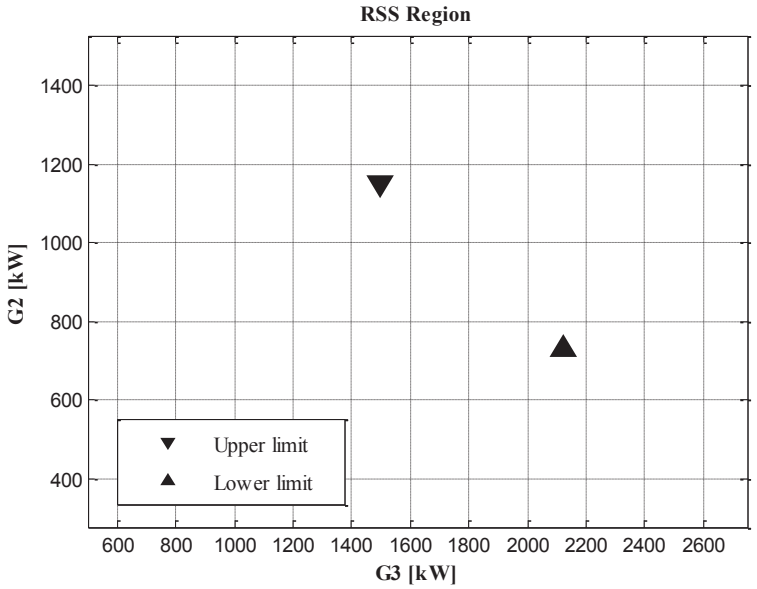

(d) Case 3

Figure 3.6. RSS regions in G_2-G_3 space

The approximated solution (d = 259) and exact solutions (d = 174) are listed in the upper and lower columns respectively in Table 3.5 and Figure 3.6(c). Although the proposed method provides values with errors, it successfully computes the more strict conditions imposed by the transmission capacity limits. The calculated values are fully acceptable from the point of view of DS balance constraints but partially optimistic with respect to line flow limits, in which the former is a strict hard constraint and the latter soft constraints in general. Thus, the proposed method is not only very promising new

technique but also very useful in order to measure the security region for power system operation due to the impact of RE penetration. In case 3 where the uncertainty is further increased, RSS disappeared where d = -141 as seen in Table 3.5 and described in Figure 3.6(d). The proposed method provides the exact solution.

The situation implies that there are no security regions to guarantee conventional N-1 security. When such a situation is encountered, it will be necessary to take actions for the preparations of additional capacity of controllable generations. The value of index d is an effective measure for the size of RSS since the positive value of d guarantees the existence of RSS region as suggested by the proposed method. The necessary amount of additional generations must be analyzed to preserve secure power system operation in this situation.

The proposed method can take into account multiple scenarios simultaneously in uncertainty vector p, and provide the size of the feasible region for all the scenarios. On the other hand, system planner usually performs analysis for a single scenario and obtains an operation planning solution at a time. In this case, they tend to face a situation in which different operation planning solutions are obtained for individual scenarios. Then, they try to find worst case operation planning solution useful for all the scenarios. In general, this is an arduous task for system planner. The proposed method is helpful to know the solution sets and the size of solution space, d. This can be a useful index to be used on-line ELD operation since its computation is very fast.

3.8. Concluding Remarks

A new problem for the evaluation of robust static security region, RSS, is proposed in order to assess the power system N-1 security against uncertainties. The proposed method computes the security region size in the controllable parameter space (generator outputs) for the specified CIs, upper and lower limits of uncertain parameters (PV outputs). A new formulation and an approximated solution are proposed based on the linear programming. It is possible by the proposed method to monitor the degree of system capability against the existing uncertainties. The formulation allows various setting of uncertainties to preserve the N-1 power system security in the system planning and operation taking into account a set of constraints in load dispatching. The proposed method is useful when the worst case scenarios are taken into account at a time, while the

conventional stochastic methods are also useful for stochastic analysis. The proposed method is not almighty and complements the existing methods.

CHAPTER 4 : ROBUST POWER SYSTEM SECURITY ASSESSMENT UNDER UNCERTAINTIES USING BI-LEVEL OPTIMIZATION

4.1. Introduction

A bi-level optimization problem becomes an active research area of mathematical programming. It constitutes a very important class of problems with various applications in different fields of engineering and applied sciences. A bi-level optimization can be seen as a multi-level problem with two-level optimization model. In general, this technique is a stage of two optimization problems including upper and lower levels. A bi-level optimization problem is a challenging class of optimization problem to be solved where the objective function at the upper level has no explicit formulation, and it is compounded by the lower level optimization problem. Consequently, the objective function in the upper-level part can be optimized by taking into account the lower-level section. In power system, the bi-level optimizations have been employed for the worst case computation such as disruptive threat [59], [60], interdiction [61], vulnerability analysis [62], and contingency ranking [63].

This chapter presents a new formulation and method which are transformed into bi-level optimization framework. A bi-level optimization approach is used to solve the robust power system security problems which refer to robust static security (RSS) and robust dynamic feasible (RDF) problems, respectively. The proposed bi-level optimization model is converted into single level optimization problem and solved using mixed integer linear programming (MILP). The proposed method is employed to solve RSS problem for static economic dispatch case studies. Then, it is used for solving RDF problem with dynamic economic dispatch. A six-bus, IEEE 14-bus, IEEE 30-bus and IEEE 118-bus power system models are used as the test system to show the efficacy of the proposed method in order to measure the security region in dynamic power system operation circumstances.

4.2. Problem Formulation

In this section, the problem formulation to compute robust power system security

region regarding static and dynamic power system operations is provided. The concept of RSS and RDF security regions is depicted in Figure 4.1. The basic concepts of RSS and RDF security regions in details were described in Chapter 2.

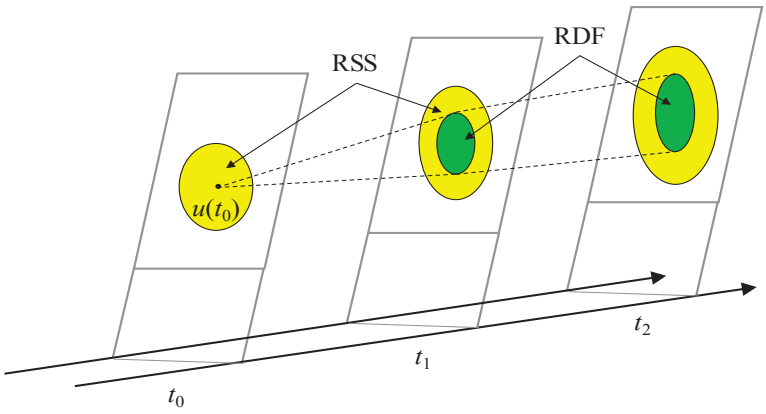

Figure 4.1. The concept of RSS and RDF security regions [56]

The feasible region of control variable u satisfying all constraints of power flow equations under load p for this study is represented in (4.1) [53].

$$\left.\begin{aligned} &SS_u(p) = \left\{u \mid SS_u^0(p) \cap SS_u^1(p) \cap \cdots \cap SS_u^N(p)\right\} \\ &SS_u^n(p) = \left\{u \mid \underline{u} \le u \le \overline{u},\ f^n = 0,\ \ g^n \le 0\right\} \\ &n = 0, 1, \cdots, N \end{aligned}\right\} \tag{4.1}$$

The equation (4.1) also can be re-written as follow,

$$SS_u(p) = \left\{u \mid H(x, u, p) \le 0\right\} \tag{4.2}$$

H is the constraint set which implies a region of u. The security region (4.1) or (4.2) is called "Static Security (SS)" region. Further explanation of this security region is described in chapter 2. By analyzing this security area, the power system state can be guaranteed to satisfy N-1 security criterion when the power system operating point exists within SS region.

In the case of multi-period power system operation, the time interval is decomposed into several periods. In reality, the generator output would require additional time to increase or decrease its power due to thermal stress. This condition is translated into a new set of constraint called ramping constraint δ, which is defined as follows.

$$-\delta \cdot (t - t_0) \le u(t) - u(t_0) \le \delta \cdot (t - t_0) \tag{4.3}$$

where δ is ramp limit of the generator, t_0 represents the current time or initial time point and each time point t_1, t_2, t_3 ... implies future time points.

The initial operating point $u(t_0)$ in this study is assumed at t_0, where a security region at each time t is reachable from the initial point t_0. The region is called dynamic feasible (DF) security region where is defined by the set of time points $u(t_1), u(t_2), .., u(t)$ satisfying constraints (4.3) and (4.4) for all t, ($t_0 < t$). Thus, DF security region is defined as

$$DF_{u(t)}(p(t)) = \{u(t) \mid H_{DF}(x(t), u(t), p(t)) \le 0, \text{ given } u(t_0)\} \tag{4.4}$$

H_{DF} is the constraint set consisting of (4.2) and (4.3) for all t, ($t_0 < t$).

Robust static security (RSS) region defined as the safe-side security region for all possible parameter variations is formulated as follows.

$$RSS_u = \{u \mid u \in \bigcap_{p \in R_p} SS_u(p)\} = \{u \mid H(x, u, p) \le 0 \text{ , for all } p \in R_p\} \tag{4.5}$$

A mathematical expression of fluctuation parameter such as load forecast is an essential component for power system operation. This parameter is expressed by $p(t)$ at time t and defined in the following form,

$$p(t) = \hat{p}(t \mid t_0) + \Delta(t \mid t_0)$$

$$\Pr\{\underline{p}(t) \le p(t) \le \overline{p}(t)\} = CL, \quad 0 \le CL \le 1 \tag{4.6}$$

where $\hat{p}(t \mid t_0)$ implies the forecast of $p(t)$ predicted at t_0, $\Delta(t \mid t_0)$ is the prediction error which concerns with "uncertainty". The confidence interval (CI) is used to characterize the uncertainty where the upper and lower bounds relate to confidence level, CL. When the forecast time t - t_0 increases, the uncertainty becomes larger. The bounds of uncertainties can be determined in this study because CL is specified. In the following expression describes the confidence intervals (CIs) of $p(t)$ at time t.

$$R_{p(t)} = \{p(t) \mid \underline{p}(t) \le p(t) \le \overline{p}(t)\} \tag{4.7}$$

$$\underline{p}(t) = \hat{p}(t \mid t_0) + \underline{\Delta}(t \mid t_0), \ \overline{p}(t) = \hat{p}(t \mid t_0) + \overline{\Delta}(t \mid t_0) \tag{4.8}$$

The expression describes that the selection value of CL can be determined regarding uncertainty Δ around the prediction $\hat{p}$. In reality, maximum forecast error in p can be set as limits of Δ. The example for setting this parameter $p(t)$ is shown in Figure

4.2. The time to carry out the prediction will be at some future point ($t = t_0$) such as at 24 hours before the real time operation. In this situation, the accuracy of prediction errors is available in advance, and reasonable values of the maximum errors can be set for each prediction time based on the historical data analysis. The confidence interval for this setting [44] is used in the proposed method to obtain the reliable result. The bounds of uncertainties (4.9) are utilized in this study.

$$\underline{\Delta}(t \mid t_0) = -\sigma \cdot (t - t_0),\ \overline{\Delta}(t \mid t_0) = \sigma \cdot (t - t_0) \tag{4.9}$$

This mathematical expression implies that uncertainties are nonexistence at $t = t_0$ and increase with respect to t for future predictions.

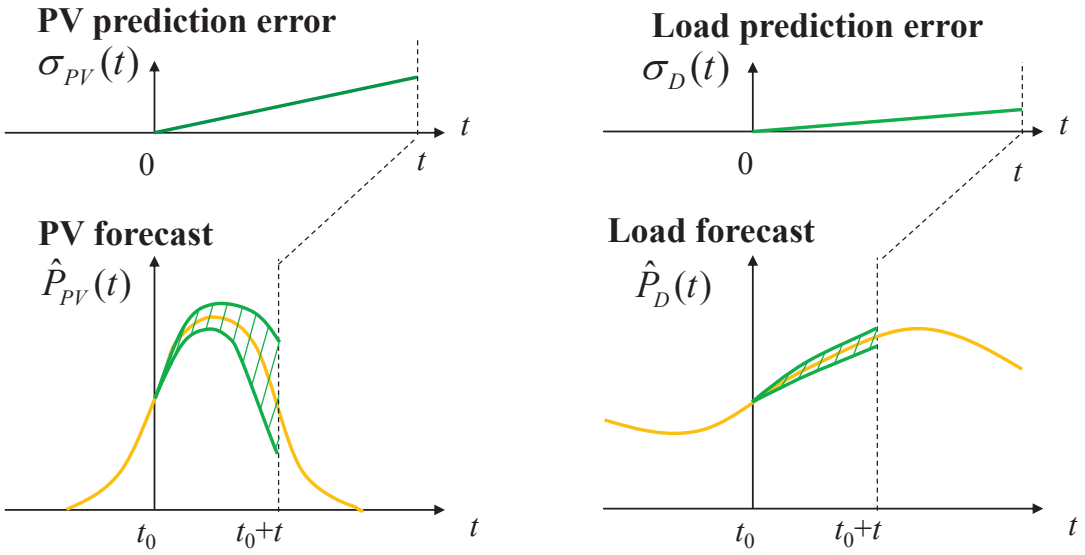

Figure 4.2. PV and load forecast conditions.

A robust dynamic feasible (RDF) security region which is used to examine the security region on each time point t reachable from initial point t_0 is defined as follows,

Robust dynamic feasible (RDF) region is defined as

$$\begin{aligned} RDF_{u(t)} &= \left\{u(t) \mid u(t) \in \bigcap_{p \in R_{p(t)}} DF_{u(t)}(p(t))\right\} \\ &= \left\{u(t) \mid H_{DF}(x(t), u(t), p(t)) \le 0, \text{ for all } p(t) \in R_{p(t)}, \text{ given } u(t_0)\right\} \end{aligned} \tag{4.10}$$

4.3. Security Region's Size Computation

In Chapter 3, the problem formulation used to solve the robust power system security issue is based on linear programming. Unfortunately, the proposed method could

not exactly measure the security region under strict transmission line limits. Therefore, an appropriate method is developed in this chapter in order to solve the robust power system security problem where it is formulated in a bi-level optimization framework and examined in several power system models. The proposed approach to obtain the upper and lower bounds of robust static security (RSS) region is provided in the following forms [56].

Upper bound (UB) :

$$\bar{\alpha}_{RSS} =: \min_{p \in Rp} \{ c^T u \} \tag{4.11}$$

Subject to $H(x,u,p) \le 0$.

$$u \in \arg\max_{u} \{c^T u\} \tag{4.12}$$

Subject to $H(x,u,p) \le 0$.

Lower bound (LB) :

$$\underline{\alpha}_{RSS} =: \max_{p \in Rp} \; c^T u \tag{4.13}$$

Subject to $H(x,u,p) \le 0$.

$$u \in \arg\min_{u} \{c^T u\} \tag{4.14}$$

Subject to $H(x,u,p) \le 0$.

Index d used to measure the diameter of security regions is defined in the following form [55, 56].

$$d = \frac{1}{\| c \|} (\bar{\alpha}_{RSS} - \underline{\alpha}_{RSS}) \tag{4.15}$$

The existence of RSS region is indicated by a positive value of index d. On the contrary, RSS is nonexistence if the indicator d value is negative. The power system can be more easily operated within RSS region when the security index d is large, and the power system security is guaranteed. The diameter d between the bounds of security region may become larger or smaller due to affected by changing the setting of normal vector c and the volume size of RSS region. When the intersection of the RSS region volume disappears, d becomes negative without exclusion. It is better to avoid the power

system operation on the edge of RSS region. When d is a negative value, it shows the worst thing occurred due to no security region exists. In this situation, some action to keep or enlarge the security region is carried out for increasing d in order to keep operating point within the security region.

In dynamic power system operation and planning, monitoring the security region is carried out by the proposed approach called RDF where constitutes the extension of the proposed formulation for RSS in static system operation. The problem is converted into discrete time point sequence, t=0, 1, 2, … with given initial point $u(0)$. The region size problem for RDF is formulated as follows [56].

Upper bound (UB) of RDF security region at t :

$$\bar{\alpha}_{RDF}(t) =: \min_{p(t)} \{ c^T u(t) \} \tag{4.16}$$

Subject to $H_{DF}(x(t), u(t), p(t)) \le 0$.

$u(t) \le u(t-1)^* + \delta$.

$\underline{p}(t) \le p(t) \le \bar{p}(t)$.

$$u(t) \in \arg\max_{u} \{ c^T u(t) \} \tag{4.17}$$

Subject to $H_{DF}(x(t), u(t), p(t)) \le 0$.

$u(t) \le u(t-1)^* + \delta$.

$\underline{p}(t) \le p(t) \le \bar{p}(t)$.

With given $u(0)$, present operating point.

$u(t-1)^*$ is the solution of (UB at t-1)

The solution of the problem is sequentially obtained from t=1, 2, 3, … The lower bound problem is formulated in the same way as follows:

Lower bound (LB) of RDF security region at t :

$$\underline{\alpha}_{RDF}(t) =: \max_{p(t)} \{ c^T u(t) \} \tag{4.18}$$

Subject to $H_{DF}(x(t), u(t), p(t)) \le 0$.

$u(t) \ge u(t-1)^{**} - \delta$.

$$\underline{p}(t) \le p(t) \le \overline{p}(t) .$$

$$u(t) \in \arg\min_{u} \{c^T u(t)\} \tag{4.19}$$

Subject to $H_{DF}(x,u,p) \le 0 .$

$$u(t) \ge u(t-1)^{**} - \delta .$$

$$\underline{p}(t) \le p(t) \le \overline{p}(t) .$$

With given $u(0)$, present operating point.

$u(t-1)^{**}$ is the solution of (LB at t-1)

The diameter d between the bounds of RDF security region is calculated in the following form which the approach is similar to calculate the index d of RSS region.

$$d(t) = \frac{1}{\| c \|} (\overline{\alpha}_{RDF}(t) - \underline{\alpha}_{RDF}(t)) \tag{4.20}$$

The fluctuation of security region by the uncertainty affects the diameter of security region as described in Chapter 3. When the forecast is very exact, the security region does not fluctuate and keep large size, where d is also large. In this circumstance, it is ensured that the operator can easily control the operating point inside the security region under all possible situations with uncertainties. Therefore, the system operation can be reliable and secure.

The problems (4.11)-(4.19) are formulated based on bi-level optimization framework and solved by the composition of successive linearization and transformation into mixed integer linear programming (MILP). The following procedures are employed to obtain the solution.

Step 1: Linearize (4.11) and (4.16) to obtain (A.1)-(A.4).

Step 2: Convert them into MILP problems (A.5)-(A.11)

Step 3: Solve the MILP problems to obtain the solutions.

If necessary, reiterate the process based on the successive linearization method. Note that the conversion into the MILP problem in step 2 is provided in the Appendix.

4.4. Application to Dynamic Economic Dispatch Problem

The dynamic economic dispatch (DED), which is extended from the static economic dispatch problem, is defined as a high dimensional complex constrained

optimization problem that determines the optimal generation from some generating units to match the predicted load demand and renewable energy output over a time interval. The proposed method based on robust dynamic feasible (RDF) security region which is applied for dynamic economic dispatch in order to satisfy deterministic security criterion is presented in this section.

4.4.1. Outline of Examinations

In this section, the possible applications of proposed method are demonstrated for the economic dispatch problem. As depicted in Figure 4.1, when t_0 is assumed as a present operating point, the feasibility of the future operating points depends on the capability of the system, future system conditions, and uncertainties. Namely, when the future predictions and maximum prediction errors available at t_0 are determined, the reliability of future system operations from the maximum dynamic performance of the system can be evaluated. The security assessment of future 24 hours operating conditions are demonstrated in this study with an operating point is assumed at t_0. A condition where load forecast and PV output forecast for 24 hours and their maximum errors are available at t_0 is considered in this chapter.

4.4.2. Dynamic Economic Dispatch Model

A linearized load dispatching problem in the form of (4.11) and (4.16) is discussed in this section. In general, there are controllable generators and uncontrollable loads and PVs in the individual nodes. The node injections include controllable and uncontrollable variables as follow.

Node Injection: $u + p, \quad u \in R^{N_B}, p \in R^{N_B}$ (4.20)

Demand & Supply balance: $e^T \cdot (u + p) = 0$ (4.21)

Line Flow Limit: $\underline{P}_{TL} \le S^{(n)} \cdot (u + p) \le \overline{P}_{TL} \quad n = 1 \ldots N$ (4.22)

Controllable generator limits: $\underline{u} \le u \le \overline{u}$ (4.23)

$R_p = \{p \mid \underline{p} \le p \le \overline{p}\}, \; p = [P_{PV}, P_D]$ (4.24)

The equations (4.20)-(4.24) appertain to a linear version of H in (4.2), where $e = [11 \ldots 1]^T$. Equation (4.22) is assumed as security limits. R_p in equation (4.24) implies

the region that the uncertain parameters exist as is exemplified by the shaded areas in Figure 4.2. In addition to the above static constraints, the ramp rate constraint is considered in the dynamic load dispatch model of H_{DF} in (4.16) and (4.18).

$$-\delta \le u(t+1) - u(t) \le \delta \tag{4.25}$$

4.4.3. Uncertainty Model

The uncertainty treatment is the most important part of the proposed approach in this thesis. In dynamic power system operation and planning, the uncertainty increases for future prediction such as 1-hour ahead, 2-hour ahead, 3-hour ahead, etc. The confidence interval is set after the variance of estimation error is obtained. The confidence interval (CI) is employed in a deterministic manner to avoid the system collapse. In this study, a computational framework to treat the uncertainties model utilizes the deterministic method.

The uncertainties in the form of (4.24) are used for PV generations and load consumptions in this study. Load and PV output predictions for 24 hours (t=1, 2, …,24) are used at t=0, current operating time. In this situation, the upper and lower limits of the prediction errors are assumed as given in the following form.

$$-\underline{\Delta}_{PV}(t \mid t_0) = \overline{\Delta}_{PV}(t \mid t_0) = \sigma_{PV} \cdot (t - t_0) \cdot \hat{P}_{PV}(t \mid t_0) \tag{4.26}$$

$$-\underline{\Delta}_{D}(t \mid t_0) = \overline{\Delta}_{D}(t \mid t_0) = \sigma_{D} \cdot (t - t_0) \cdot \hat{P}_{D}(t \mid t_0) \tag{4.27}$$

where $\overline{\Delta}_{PV}(t \mid t_0)$, $\underline{\Delta}_{PV}(t \mid t_0)$, $\overline{\Delta}_{D}(t)$, $\underline{\Delta}_{D}(t)$: upper and lower bounds of PV and load prediction errors for 24 hours (t=1, 2,…,24) which are evaluated at t_0. Coefficients $\sigma_{PV}(t)$, $\sigma_{D}(t)$ represent prediction accuracies. The equations imply that the prediction errors increase for the more future forecast as provided in Figures 4.2 and 4.3.

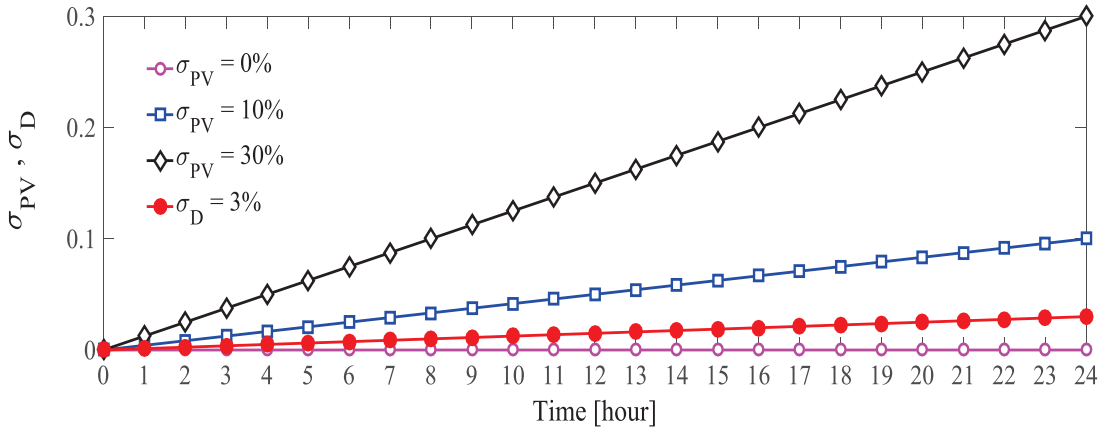

Figure 4.3. Maximum prediction error $\sigma(t)$

4.4.4 Numerical Examples of Feasibility Region

The maximization problem of security region in dynamic power system operation circumstance is implied by objective (4.16) with constraints (4.20)-(4.25), where the decision variables are *u* and *p* for *t*=1..24. Inputs are their upper and lower bounds, while outputs are the optimal *u* for the worst case of *p* inside the bound pre-specified by (4.26)-(4.27). The minimization is the same except for objective (4.18). After the optimizations, *d* is obtained. If *d* is very small, possible actions are carried out to increase the value of *d* by relaxing the active constraints which are provided by the results of the optimizations. The actions consist of additional power supply at the constrained node, demand response, curtailment of PV output, load shedding, etc.

The different problems can be analyzed by selecting the normal vector $c = [c_1 c_2 \cdots c_{NB}]^T$ in the objective as follows.

1) Production cost setting:

When the generator cost coefficients are defined, the lower bound solution presents the worst case economic operating point against uncertainties, while *d* denote the size of feasibility region quantified in MW. The solution with positive *d* ensures the secure power system operation.

2) Total power supply setting:

By setting c_i = 1 for generators, and 0 for slack and other buses, the objective appertains to the total generation.

$$cu = \sum_{i \in GeneratorBus} u_i \tag{4.28}$$

This case directly analyzes the adequacy of total power supply.

The proposed method is examined using small-scale power system model including 3-generator, 3-PV generation unit and 3-load demand [55]. In here, the simulation results only depict the computation in order to confirm the validity and the accuracy of the proposed method.

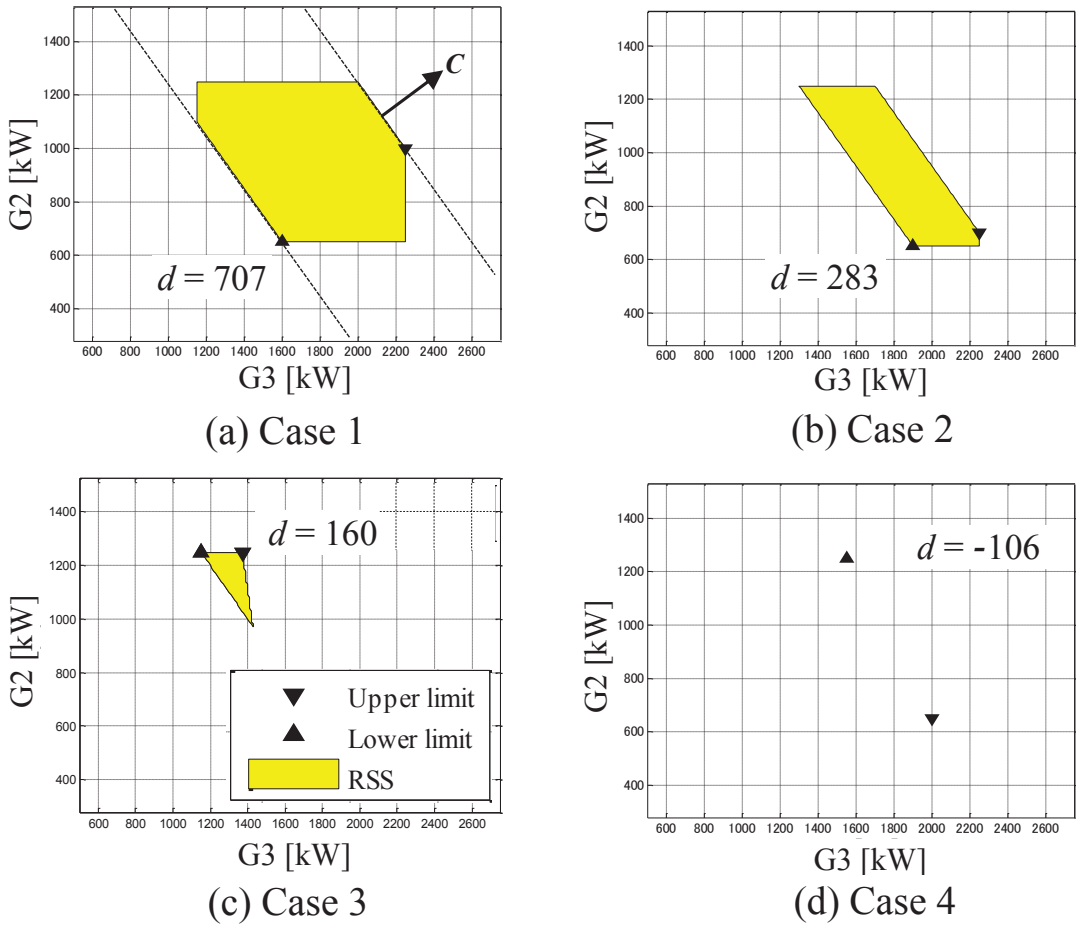

Figure 4.4. RSS region in G_2-G_3 output space

Figure 4.4. (a), Figure 4.4. (b), Figure 4.4. (c) and Figure 4.4. (d) show the feasibility regions of RSS for different sizes of uncertainties. The region shrinks as the uncertainty increases. The triangle points indicate the upper and lower bounds computed by the proposed method, which provides the region size accurately.

4.4.5. Six-Bus System Example

A six-bus test system illustrated in Figure 4.5 is used in this section to demonstrate 24-hour robust power system security assessment based on the proposed approach. The six-bus system data are listed in Table 4.1-4.3 and cited from [63], [64], including ramp-rate data and the daily total load data provided in Figure 4.6. The slack generator capacity (85MW) and PV generation unit are installed on buses 4 and 3, respectively. The power system model includes 4-generator unit, 3-load demand, and 1-PV generation source. PV data is especially taken from "the 2006 National Renewable Energy Laboratory (NREL) data set" [65]. The PV data is shown in Figure 4.7. Two cases are used to examine the robustness of the proposed method.

Case 1: PV capacity is 74MW (28.9% of peak load 256MW).

Case 2: PV capacity is 125MW (48.8% of peak load 256MW).

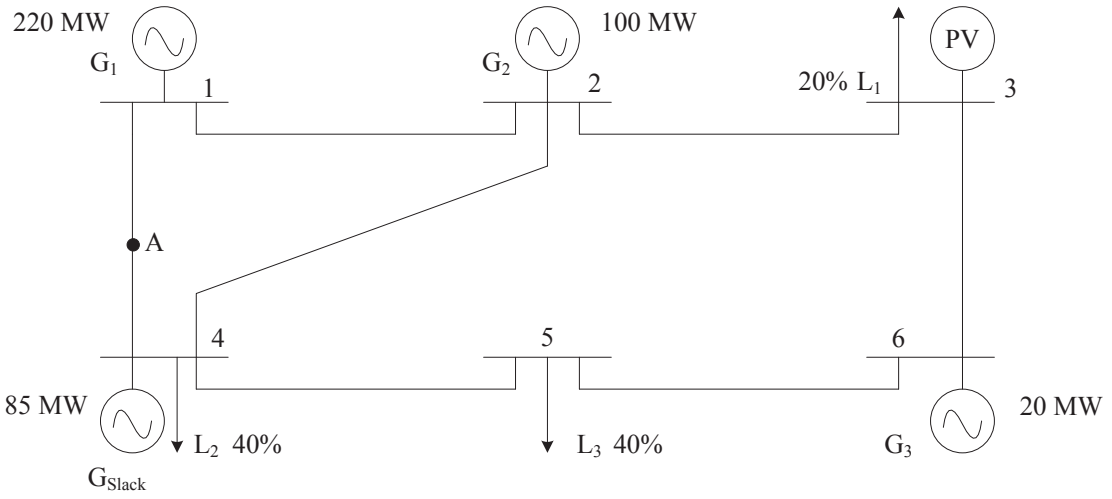

Figure 4.5. Six-bus test system

Table 4.1. Generator data for six-bus model

Generator	Bus No.	Pmax (MW)	Pmin (MW)	Ramp (MW/h)
G_1	1	220	100	55
G_2	2	100	10	50
G_3	6	20	10	20

Table 4.2. Transmission line data for six-bus model

Line No.	From Bus	To Bus	R (pu)	X (pu)	Flow Limit (MW)
1	1	2	0.0050	0.170	200
2	1	4	0.0030	0.258	100
3	2	4	0.0070	0.197	100
4	5	6	0.0020	0.140	100
5	3	6	0.0005	0.018	100

Table 4.3. Bus load distribution profile for six-bus model

Load	At Bus	Load Ratio
1	1	0.2
2	2	0.4
3	3	0.4

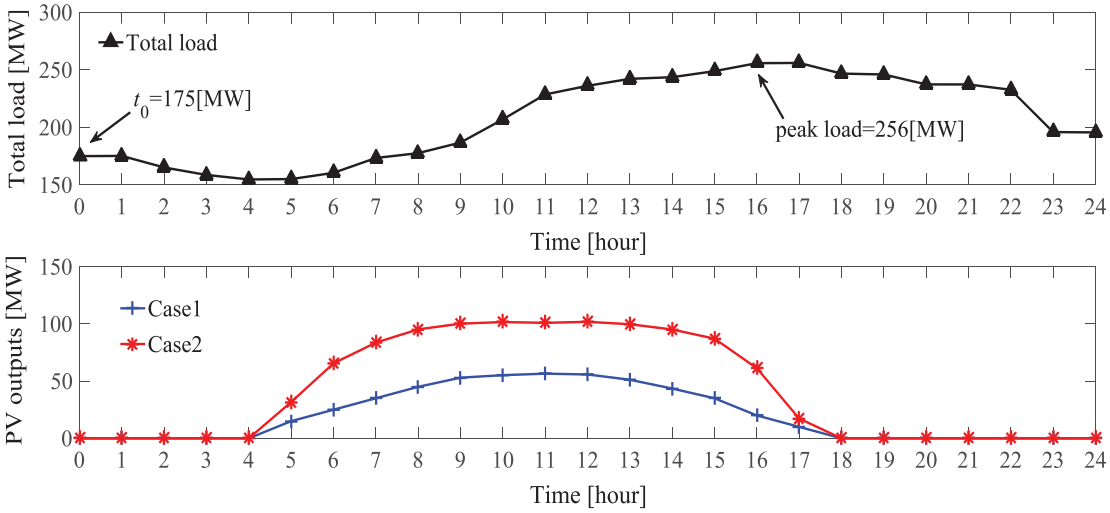

Figure 4.6. Hourly total load and PV data for six-bus model

Single line outage of double circuits lines is assumed as a contingency at point A between buses 1 and 4 in Figure 4.5. First, a conventional static economic dispatch approach is employed to obtain the initial operating point at t_0. The total load at t_0 is 175MW with load distribution 20% at bus 3, 40% at buses 4 and 5, which are varied proportionally with time. Next, the proposed problems are solved to compute the $\underline{\alpha}_{RDF}$, $\overline{\alpha}_{RDF}$ with the production cost setting to obtain Figure 4.7. The result appertains to forecast errors of $\sigma_{PV} = 30\%$, $\sigma_D = 3\%$ in case 2.

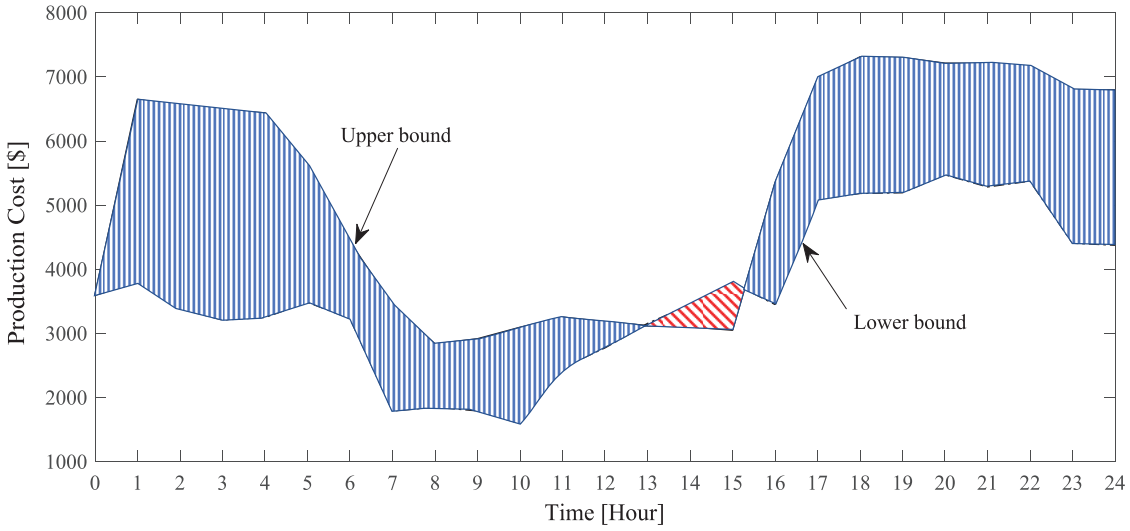

Figure 4.7. The bounds of feasibility region with production cost setting; the lower bound indicates the worst case economic operation

For this figure, the abscissa is the time point t at 0, 1, 2, .. , 24 o'clock, where t = 0 is the current time at which the load and PV output predictions are conducted for 24 hours. The lower bound of RDF $\underline{\alpha}_{RDF}$ with the production cost setting expresses the recommended secure operation pattern while the upper bound of the feasible region $\bar{\alpha}_{RDF}$ is guaranteeing the security criterion. Noted that the reverse of $\underline{\alpha}_{RDF}$ and $\bar{\alpha}_{RDF}$ is observed at around at 14:00 o'clock. This condition interprets that the operation itself is possible, but the operating point is not inside the security region since the region itself disappears. Figure 4.8 shows the same computation with the total power supply setting. This setting can directly measure the flexibility of the total power supply. The region between $\underline{\alpha}_{RDF}$ and $\bar{\alpha}_{RDF}$, blue colored area, is the feasible region with positive d. We can observe the same result as before that the system operation is not secure at around 14:00 o'clock with negative d. Demand-supply balance is not guaranteed in these time periods depending on conditions of PV generations and loads.

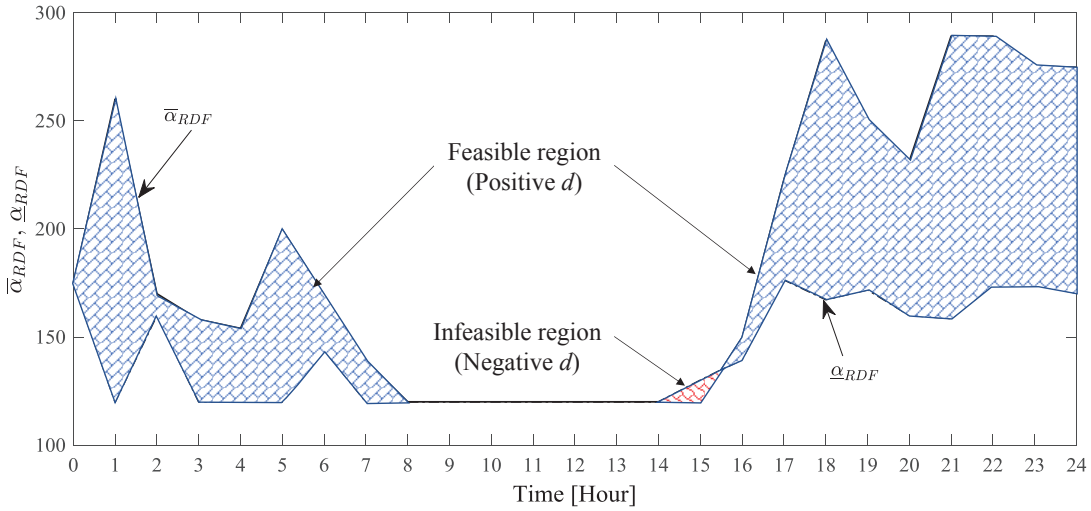

Figure 4.8. The bounds of feasibility region with total power supply setting; Reverse of upper and lower bounds indicates infeasibility

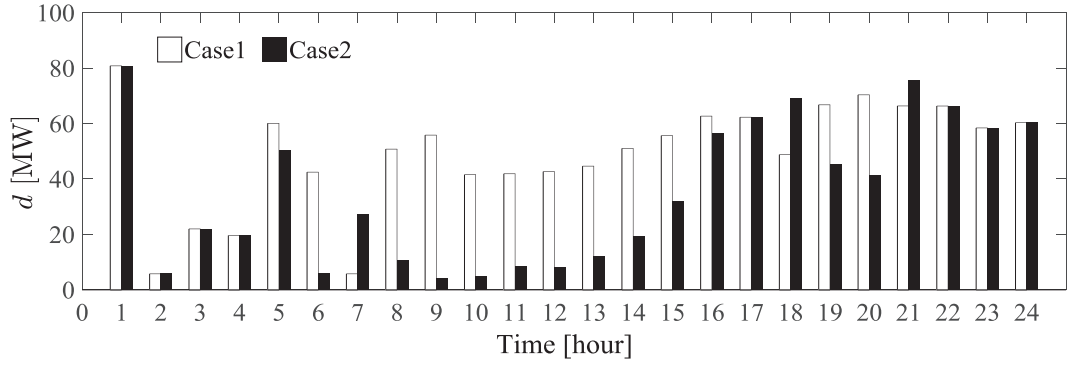

(a) $\sigma_{PV} = 0\%, \sigma_D = 3\%$

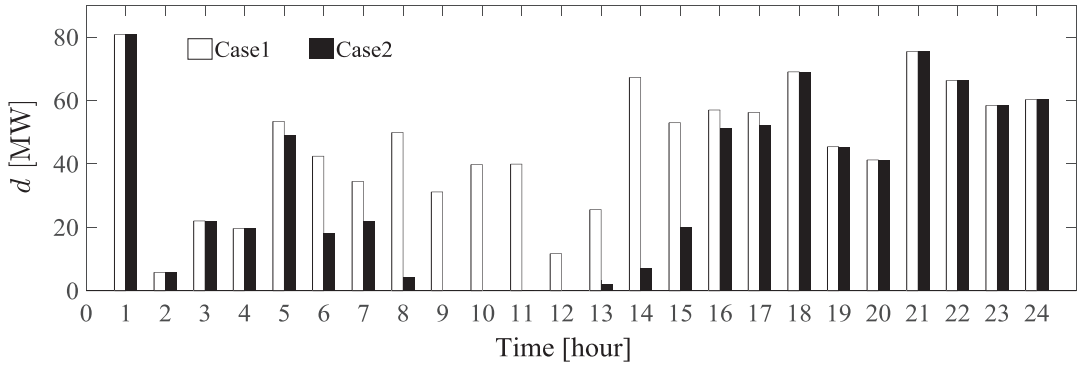

(b) $\sigma_{PV} = 10\%, \sigma_D = 3\%$

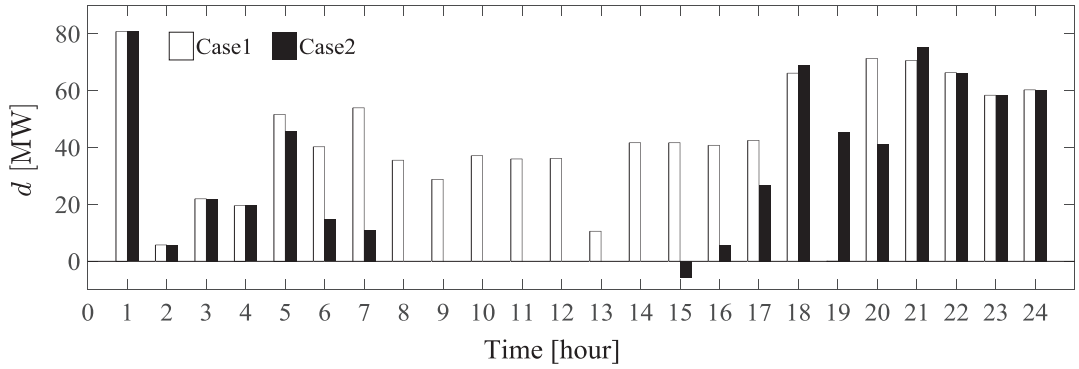

(c) $\sigma_{PV} = 30\%, \sigma_D = 3\%$

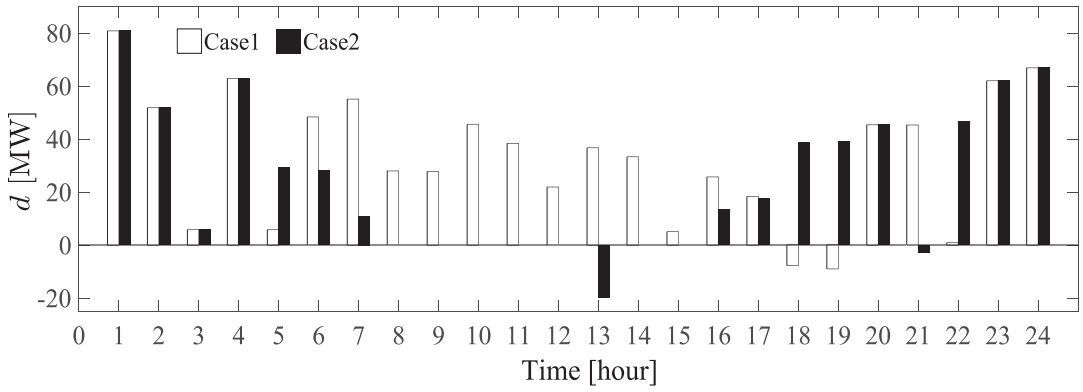

(d) $\sigma_{PV} = 30\%, \sigma_D = 3\%$ and N-1 contingency

Figure 4.9. Size of feasibility region *d* measured in MW; Negative values indicate possible power mismatch in the worst case

Distance *d* is a useful security index representing the size of the security region as observed in Figures 4.9(a)-(d), where the system operation is easier for a greater *d*. Figures 4.9 (a)-(d) show security index *d* of RDF for different conditions of PV predictions. The white bars imply *d* for case 1 and black bars for case 2. When the forecast is very exact, *d* is large as seen in Figure 4.9. (a) as expected by theoretical point of view.

When the load and PV predictions have degenerated, *d* tends to become small and sometimes negative, where the robust security cannot be guaranteed as observed in Figures 4.9. (b), (c) and (d). It is needless to say that the indicator *d* for case 1 and 2 is similar during a night when PV outputs are zero: the distance *d* shows large values since PV uncertainties are nonexistence.

4.4.6. IEEE 14-Bus System Example

A modified IEEE 14-bus system including five generators, 20 branches, and 11 loads as shown in Figure 4.10 is used to examine the proposed method. The system data

are cited from [66], and the hourly total load and PV output data are provided in Figure 4.11. The ramp-rate of the generator is set as 3% of upper generator limit. The slack generator capacity (92.5MW) is installed at bus 13.

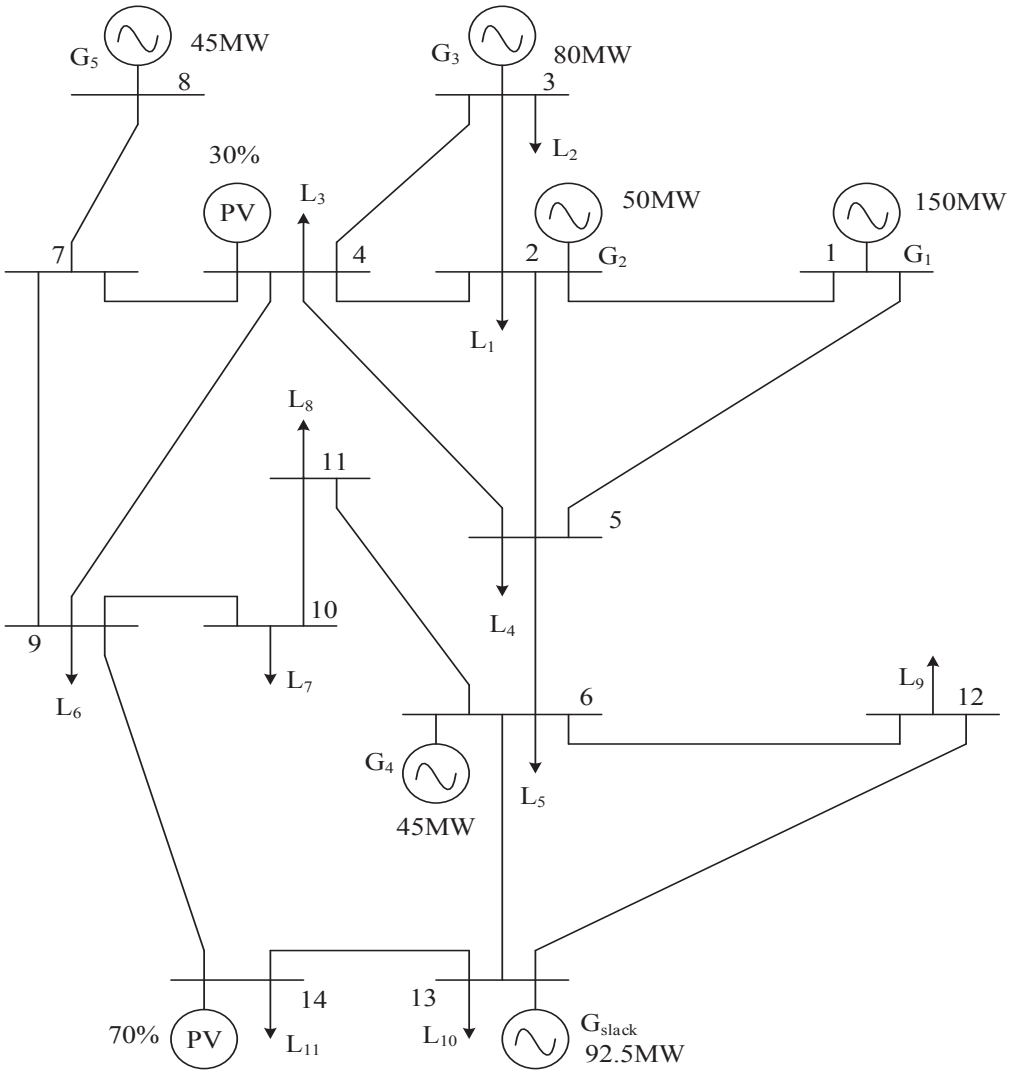

Figure 4.10. A modified IEEE 14-bus system.

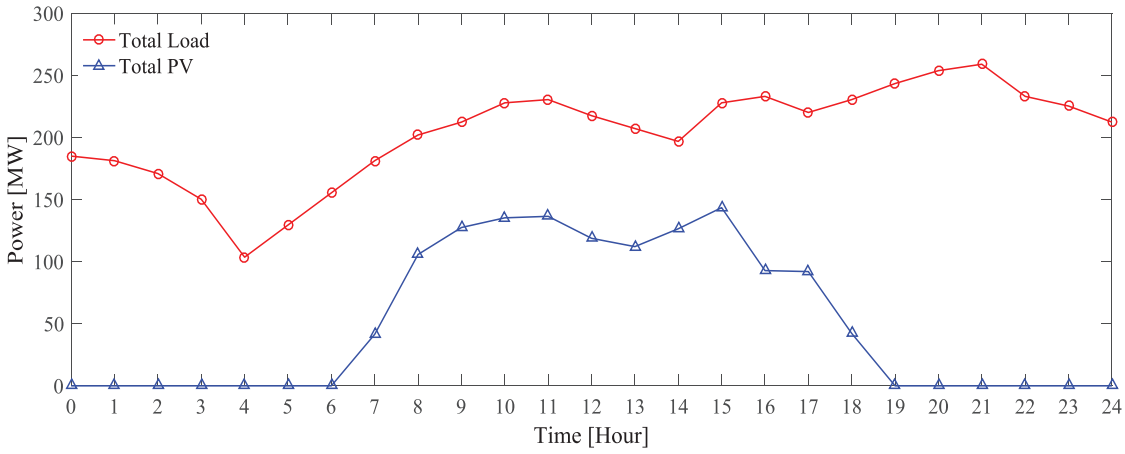

Figure 4.11. Hourly total load and PV output data for IEEE 14-bus system

The total PV installed capacity is 202 MW where distributed 30% at bus 4 and 70% at bus 14. Base load at t_0 is 185 MW. Generator data, transmission line data, and distribution factors of loads at different buses are listed in Tables 4.4 – 4.6. The hourly PV output data to test the robustness of the proposed method is collected from [65]. To evaluate the RDF security region, the following cases are studied.

Case 1: $\sigma_{PV} = 0\%, \sigma_D = 0\%$, Case 2: $\sigma_{PV} = 10\%, \sigma_D = 3\%$,

Case 3: $\sigma_{PV} = 30\%, \sigma_D = 5\%$, Case 4: Case 3 with line fault between bus 1 and 5.

Table 4.4. IEEE 14-bus's generator data

Generator	Bus No.	Pmax (MW)	Pmin (MW)
G_1	1	150	50
G_2	2	50	20
G_3	3	80	12
G_4	6	45	10
G_5	8	45	10

Table 4.5. IEEE 14-bus's transmission line data

Line No.	From Bus	To Bus	R (pu)	X (pu)	Flow Limit (MW)
1	1	2	0.01938	0.05917	50
2	1	5	0.05403	0.22304	65
3	2	3	0.04699	0.19797	60
4	2	4	0.05811	0.17632	60
5	2	5	0.05695	0.17388	60
6	3	4	0.06701	0.17103	60
7	4	5	0.01335	0.04211	40
8	4	7	0	0.20912	65
9	4	9	0	0.55618	40
10	5	6	0	0.25202	65
11	6	11	0.09498	0.1989	50
12	6	12	0.12291	0.25581	50
13	6	13	0.06615	0.13027	50
14	7	8	0	0.17615	50

Table 4.5. IEEE 14-bus's transmission line data (cont'd)

Line No.	From Bus	To Bus	R (pu)	X (pu)	Flow Limit (MW)
15	7	9	0	0.11001	30
16	9	10	0.03181	0.0845	50
17	9	14	0.12711	0.27038	50
18	10	11	0.08205	0.19207	50
19	12	13	0.22092	0.19988	50
20	13	14	0.17093	0.34802	50

Table 4.6. Distribution factors of loads at different buses for IEEE 14-bus

Load	At Bus	Load Factor
1	2	0.0838
2	3	0.3637
3	4	0.1846
4	5	0.0293
5	6	0.0432
6	9	0.1139
7	10	0.0347
8	11	0.0135
9	12	0.0236
10	13	0.0521
11	14	0.0575

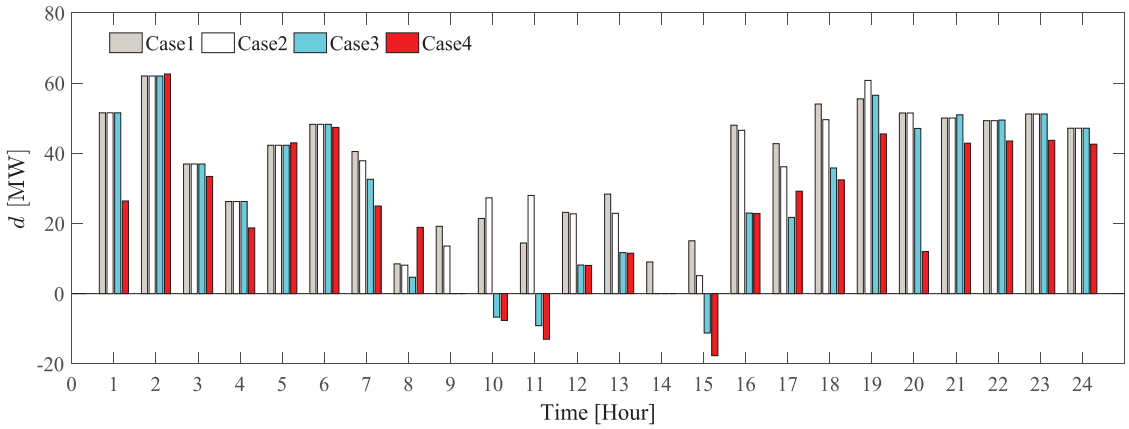

Figure 4.12. The indicator *d* of RDF security region for IEEE 14-bus system

The security index *d*, expressing the distance between the bounds of RDF security region, is described in Figure 4.12. As illustrated using graph visualization in Figure 4.12, the greater security index *d* is achieved, the easier power system operation can be controlled by the system operator. During interval times 01:00-07:00 and 18:00-24:00 for all cases, the power system operation is worthy and safe under uncertainties circumstances. However, power system operation around 08:00; 09:00; 14:00 with small *d* and 10:00; 11:00; 15:00 with negative *d* becomes main attention to be contemplated by system operator since the security region can not be ascertained in these circumstances. The power balance between demand and supply is not guaranteed due to affected by the conditions of PV outputs and loads in these time periods. If the security index value of *d* is large as illustrated in Figure 4.12 for case 1, the accuracy of PV output and load forecasts are very high, where the power system operation is feasible and existing inside security region. The security index *d* gets into smaller value and even negative due to inaccurate predictions of PV output and load as described in Figure 4.12 for case 3 and case 4, where the RDF security region shrinks. It can be concluded that indicator *d* as the diameter of robust power system security bounds is worthwhile to express the size of security region, where power system operation is easier for a greater value of *d*.

4.4.7. IEEE 30-Bus System Example

IEEE 30-bus model depicted in Figure 4.13 is used to perform the effectiveness of proposed approach. The power system model consists of 6 generators, 21 loads, 41 transmission lines and four PV generation units. The system data are taken from [67], and the daily total load and PV output data are given in Figure 4.14. Generator's ramp-rate is set to 3% of upper generator limit. The slack generator capacity (108.75MW) is added at bus 9. The total PV installed capacity is 126 MW where distributed 25% at bus 4, 25% at bus 6, 25% at bus 21 and 25% at bus 30. Base load at t_0 is 283.4 MW. Generator data, transmission line data, and distribution factors of loads at different buses are listed in Tables 4.7 – 4.9. The hourly PV data are taken from [65]. The following cases are studied to evaluate the RDF security region.

Case 1: $\sigma_{PV} = 0\%, \sigma_D = 3\%$, Case 2: $\sigma_{PV} = 10\%, \sigma_D = 3\%$,

Case 3: $\sigma_{PV} = 30\%, \sigma_D = 3\%$, Case 4: Case 3 with line fault assumed at point A.

Table 4.7. Generator data for IEEE 30-bus model

Generator	Bus No.	Pmax (MW)	Pmin (MW)
G_1	1	200	50
G_2	2	80	20
G_3	5	50	15
G_4	8	35	10
G_5	11	30	10
G_6	13	40	12

Table 4.8. Transmission line data for IEEE 30-bus model

Line No.	From Bus	To Bus	R (pu)	X (pu)	Flow Limit (MW)
1	1	2	0.02	0.06	130
2	1	3	0.05	0.19	130
3	2	4	0.06	0.17	65
4	3	4	0.01	0.04	130
5	2	5	0.05	0.2	130
6	2	6	0.06	0.18	65
7	4	6	0.01	0.04	90
8	5	7	0.05	0.12	70
9	6	7	0.03	0.08	130
10	6	8	0.01	0.04	32
11	6	9	0	0.21	65
12	6	10	0	0.56	32
13	9	11	0	0.21	65
14	9	10	0	0.11	65
15	4	12	0	0.26	65
16	12	13	0	0.14	65
17	12	14	0.12	0.26	32
18	12	15	0.07	0.13	32

Table 4.8. Transmission line data for IEEE 30-bus model (cont'd)

Line No.	From Bus	To Bus	R (pu)	X (pu)	Flow Limit (MW)
19	12	16	0.09	0.2	32
20	14	15	0.22	0.2	16
21	16	17	0.08	0.19	16
22	15	18	0.11	0.22	16
23	18	19	0.06	0.13	16
24	19	20	0.03	0.07	32
25	10	20	0.09	0.21	32
26	10	17	0.03	0.08	32
27	10	21	0.03	0.07	32
28	10	22	0.07	0.15	32
29	21	22	0.01	0.02	32
30	15	23	0.1	0.2	16
31	22	24	0.12	0.18	16
32	23	24	0.13	0.27	16
33	24	25	0.19	0.33	16
34	25	26	0.25	0.38	16
35	25	27	0.11	0.21	16
36	28	27	0	0.4	65
37	27	29	0.22	0.42	16
38	27	30	0.32	0.6	16
39	29	30	0.24	0.45	16
40	8	28	0.06	0.2	32
41	6	28	0.02	0.06	32

Table 4.9. Bus load distribution profile for IEEE 30-bus

Load	At Bus	Load Factor
1	2	7.657022
2	3	0.84686
3	4	2.681722
4	5	33.23924

Table 4.9. Bus Load Distribution Profile for IEEE 30-bus (cont'd)

Load	At Bus	Load Factor
5	7	8.045166
6	8	10.58574
7	10	2.046577
8	12	3.952011
9	14	2.187721
10	15	2.893437
11	16	1.235004
12	17	3.175723
13	18	1.129146
14	19	3.352152
15	20	0.776288
16	21	6.175018
17	23	1.129146
18	24	3.069866
19	26	1.235004
20	29	0.84686
21	30	3.740296

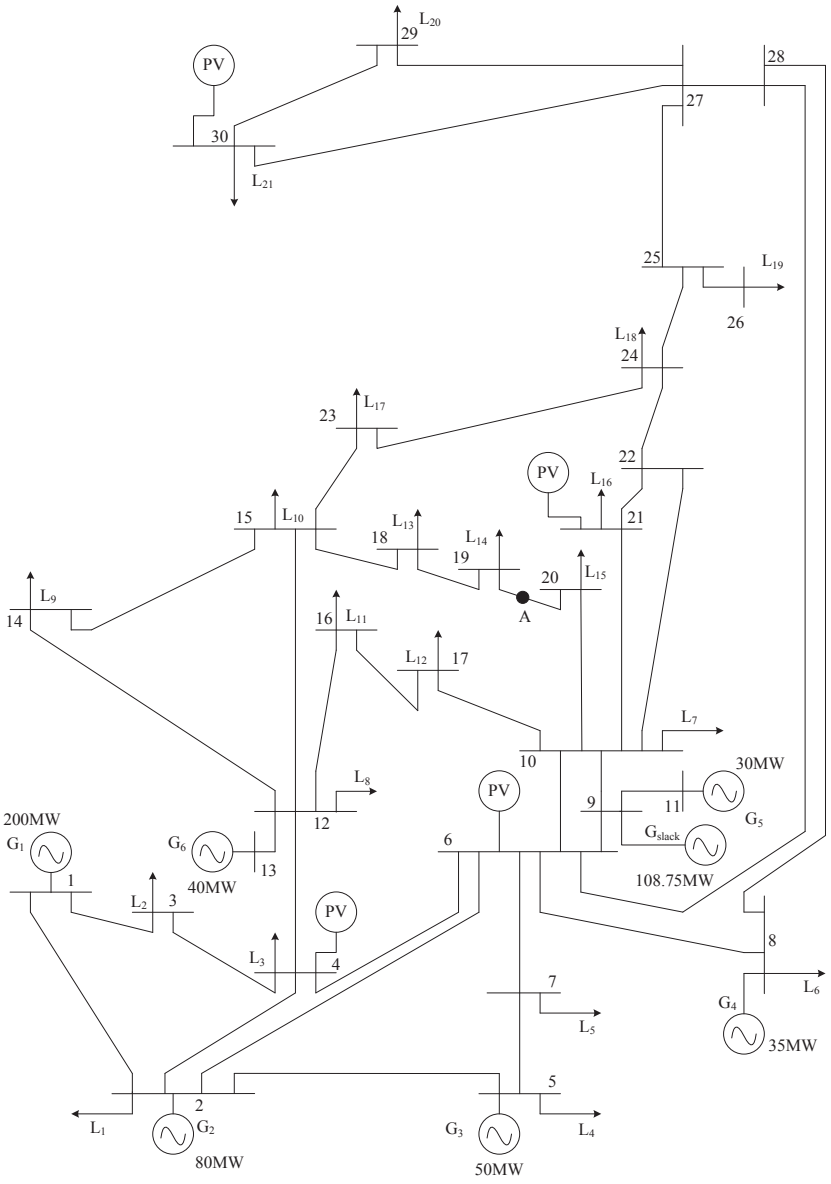

Figure 4.13. A modified IEEE 30-bus system

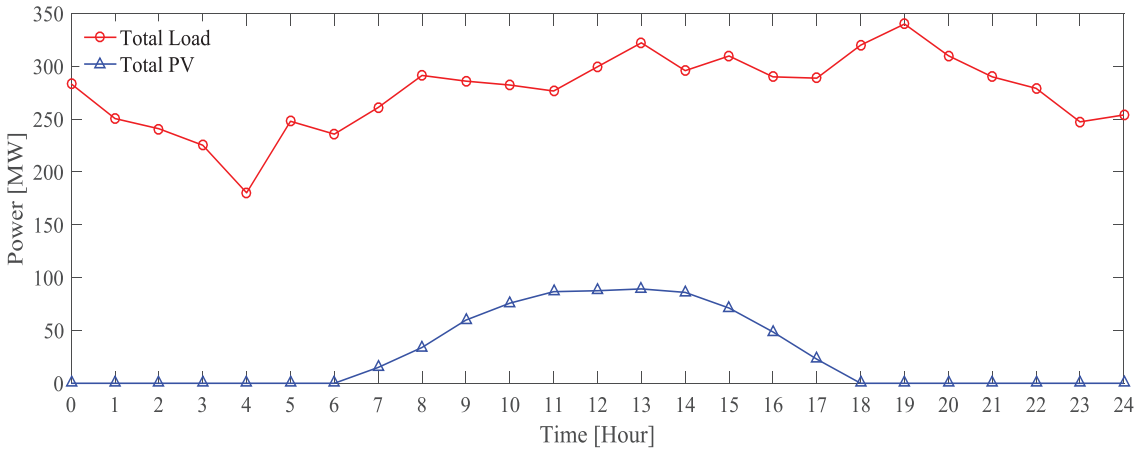

Figure 4.14. Daily total load and PV output data for IEEE 30-bus system model

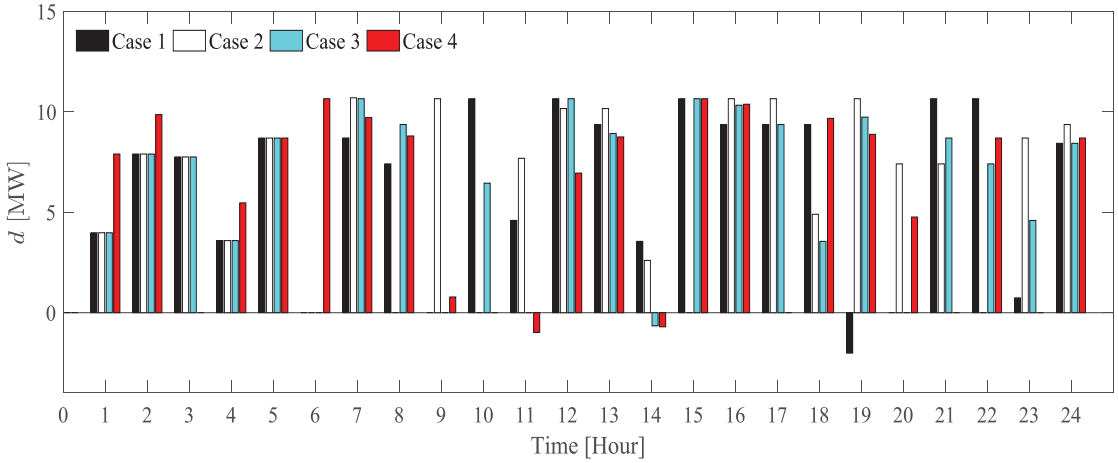

Figure 4.15. The security index *d* of RDF security region for IEEE 30-bus system model

Some following conditions are observed from Figure 4.15 : during specific time intervals 1:00-05:00 and 20:00-24:00, security index *d* is large, where power system operation is safe and reliable for all case studies. While power system operation at 11:00; 14:00 and 19.00; is not guaranteed since the existence of robust power system security disappears in these time intervals indicated by the negative value of *d*. The security indicator has great value as the exactness of PV output, and load predictions are very high. When the forecast errors of PV output and load increase, the security index *d* becomes very small and negative since the RDF security region shrinks.

4.4.8. IEEE 118-Bus System Example

To examine the efficacy of security index *d*, a modified IEEE 118-bus test system is used. The power system model includes 54 generators, 186 transmission lines, and 91 loads. The IEEE 118-bus power system model data is provided in [68]. The total load at t_0 and peak load are 3733 MW and 4080 MW, respectively. The total load and PV data for 24 hours are depicted in Figure 4.16. (a)-(b). The slack generator is located at bus 30 whose capacity is 1805MW. Generator data, transmission line data, and distribution factors of loads at different buses are listed in Tables 4.10 – 4.12. The PV installations are distributed into five areas given in Table 4.15 and cited from [65]. Two cases are employed by changing the amount of PV installation capacities to examine the performance of the proposed method as follows.

Case 1: 722 MW PV capacity (17.69% of peak load).

Case 2: 1262 MW PV capacity (30.93% of peak load).

Table 4.10. IEEE 118-bus's generator data

Generator	Bus No.	Pmax (MW)	Pmin (MW)	Ramp (MW/h)
1	4	30	5	15
2	6	30	5	15
3	8	30	5	15
4	10	300	150	150
5	12	300	100	150
6	15	30	10	15
7	18	100	25	50
8	19	30	5	15
9	24	30	5	15
10	25	300	100	150
11	26	350	100	175
12	27	30	8	15
13	31	30	8	15
14	32	100	25	50
15	34	30	8	15
16	36	100	25	50
17	40	30	8	15
18	42	30	8	15
19	46	100	25	50
20	49	250	50	125
21	54	250	50	125
22	55	100	25	50
23	56	100	25	50
24	59	200	50	100
25	61	200	50	100
26	62	100	25	50
27	65	420	100	210

Table 4.10. IEEE 118-bus's generator data (cont'd)

Generator	Bus No.	Pmax (MW)	Pmin (MW)	Ramp (MW/h)
28	66	420	100	210
29	69	300	80	150
30	70	80	30	40
31	72	30	10	15
32	73	30	5	15
33	74	20	5	10
34	76	100	25	50
35	77	100	25	50
36	80	300	150	150
37	82	100	25	50
38	85	30	10	15
39	87	300	100	150
40	89	200	50	100
41	90	20	8	10
42	91	50	20	25
43	92	300	100	150
44	99	300	100	150
45	100	300	100	150
46	103	20	8	10
47	104	100	25	50
48	105	100	25	50
49	107	20	8	10
50	110	50	25	25
51	111	100	25	50
52	112	100	25	50
53	113	100	25	50
54	116	50	25	25

Table 4.11. IEEE 118-bus's transmission line data

Line No.	From Bus	To Bus	R (pu)	X (pu)	Flow Limit (MW)
1	1	2	0.0303	0.0999	175
2	1	3	0.0129	0.0424	175
3	4	5	0.00176	0.00798	500
4	3	5	0.0241	0.108	175
5	5	6	0.0119	0.054	175
6	6	7	0.00459	0.0208	175
7	8	9	0.00244	0.0305	500
8	8	5	0	0.0267	500
9	9	10	0.00258	0.0322	500
10	4	11	0.0209	0.0688	175
11	5	11	0.0203	0.0682	175
12	11	12	0.00595	0.0196	175
13	2	12	0.0187	0.0616	175
14	3	12	0.0484	0.16	175
15	7	12	0.00862	0.034	175
16	11	13	0.02225	0.0731	175
17	12	14	0.0215	0.0707	175
18	13	15	0.0744	0.2444	175
19	14	15	0.0595	0.195	175
20	12	16	0.0212	0.0834	175
21	15	17	0.0132	0.0437	500
22	16	17	0.0454	0.1801	175
23	17	18	0.0123	0.0505	175
24	18	19	0.01119	0.0493	175
25	19	20	0.0252	0.117	175
26	15	19	0.012	0.0394	175
27	20	21	0.0183	0.0849	175
28	21	22	0.0209	0.097	175
29	22	23	0.0342	0.159	175
30	23	24	0.0135	0.0492	175
31	23	25	0.0156	0.08	500

Table 4.11. IEEE 118-bus's transmission line data (cont'd)

Line No.	From Bus	To Bus	R (pu)	X (pu)	Flow Limit (MW)
32	26	25	0	0.0382	500
33	25	27	0.0318	0.163	500
34	27	28	0.01913	0.0855	175
35	28	29	0.0237	0.0943	175
36	30	17	0	0.0388	500
37	8	30	0.00431	0.0504	175
38	26	30	0.00799	0.086	500
39	17	31	0.0474	0.1563	175
40	29	31	0.0108	0.0331	175
41	23	32	0.0317	0.1153	140
42	31	32	0.0298	0.0985	175
43	27	32	0.0229	0.0755	175
44	15	33	0.038	0.1244	175
45	19	34	0.0752	0.247	175
46	35	36	0.00224	0.0102	175
47	35	37	0.011	0.0497	175
48	33	37	0.0415	0.142	175
49	34	36	0.00871	0.0268	175
50	34	37	0.00256	0.0094	500
51	38	37	0	0.0375	500
52	37	39	0.0321	0.106	175
53	37	40	0.0593	0.168	175
54	30	38	0.00464	0.054	175
55	39	40	0.0184	0.0605	175
56	40	41	0.0145	0.0487	175
57	40	42	0.0555	0.183	175
58	41	42	0.041	0.135	175
59	43	44	0.0608	0.2454	175
60	34	43	0.0413	0.1681	175
61	44	45	0.0224	0.0901	175
62	45	46	0.04	0.1356	175

Table 4.11. IEEE 118-bus's transmission line data (cont'd)

Line No.	From Bus	To Bus	R (pu)	X (pu)	Flow Limit (MW)
63	46	47	0.038	0.127	175
64	46	48	0.0601	0.189	175
65	47	49	0.0191	0.0625	175
66	42	49	0.0715	0.323	175
67	42	49	0.0715	0.323	175
68	45	49	0.0684	0.186	175
69	48	49	0.0179	0.0505	175
70	49	50	0.0267	0.0752	175
71	49	51	0.0486	0.137	175
72	51	52	0.0203	0.0588	175
73	52	53	0.0405	0.1635	175
74	53	54	0.0263	0.122	175
75	49	54	0.073	0.289	175
76	49	54	0.0869	0.291	175
77	54	55	0.0169	0.0707	175
78	54	56	0.00275	0.00955	175
79	55	56	0.00488	0.0151	175
80	56	57	0.0343	0.0966	175
81	50	57	0.0474	0.134	175
82	56	58	0.0343	0.0966	175
83	51	58	0.0255	0.0719	175
84	54	59	0.0503	0.2293	175
85	56	59	0.0825	0.251	175
86	56	59	0.0803	0.239	175
87	55	59	0.04739	0.2158	175
88	59	60	0.0317	0.145	175
89	59	61	0.0328	0.15	175
90	60	61	0.00264	0.0135	500
91	60	62	0.0123	0.0561	175
92	61	62	0.00824	0.0376	175
93	63	59	0	0.0386	500

Table 4.11. IEEE 118-bus's transmission line data (cont'd)

Line No.	From Bus	To Bus	R (pu)	X (pu)	Flow Limit (MW)
94	63	64	0.00172	0.02	500
95	64	61	0	0.0268	500
96	38	65	0.00901	0.0986	500
97	64	65	0.00269	0.0302	500
98	49	66	0.018	0.0919	500
99	49	66	0.018	0.0919	500
100	62	66	0.0482	0.218	175
101	62	67	0.0258	0.117	175
102	65	66	0	0.037	500
103	66	67	0.0224	0.1015	175
104	65	68	0.00138	0.016	500
105	47	69	0.0844	0.2778	175
106	49	69	0.0985	0.324	175
107	68	69	0	0.037	500
108	69	70	0.03	0.127	500
109	24	70	0.00221	0.4115	175
110	70	71	0.00882	0.0355	175
111	24	72	0.0488	0.196	175
112	71	72	0.0446	0.18	175
113	71	73	0.00866	0.0454	175
114	70	74	0.0401	0.1323	175
115	70	75	0.0428	0.141	175
116	69	75	0.0405	0.122	500
117	74	75	0.0123	0.0406	175
118	76	77	0.0444	0.148	175
119	69	77	0.0309	0.101	175
120	75	77	0.0601	0.1999	175
121	77	78	0.00376	0.0124	175
122	78	79	0.00546	0.0244	175
123	77	80	0.017	0.0485	500
124	77	80	0.0294	0.105	500

Table 4.11. IEEE 118-bus's transmission line data (cont'd)

Line No.	From Bus	To Bus	R (pu)	X (pu)	Flow Limit (MW)
125	79	80	0.0156	0.0704	175
126	68	81	0.00175	0.0202	500
127	81	80	0	0.037	500
128	77	82	0.0298	0.0853	200
129	82	83	0.0112	0.03665	200
130	83	84	0.0625	0.132	175
131	83	85	0.043	0.148	175
132	84	85	0.0302	0.0641	175
133	85	86	0.035	0.123	500
134	86	87	0.02828	0.2074	500
135	85	88	0.02	0.102	175
136	85	89	0.0239	0.173	175
137	88	89	0.0139	0.0712	500
138	89	90	0.0518	0.188	500
139	89	90	0.0238	0.0997	500
140	90	91	0.0254	0.0836	175
141	89	92	0.0099	0.0505	500
142	89	92	0.0393	0.1581	500
143	91	92	0.0387	0.1272	175
144	92	93	0.0258	0.0848	175
145	92	94	0.0481	0.158	175
146	93	94	0.0223	0.0732	175
147	94	95	0.0132	0.0434	175
148	80	96	0.0356	0.182	175
149	82	96	0.0162	0.053	175
150	94	96	0.0269	0.0869	175
151	80	97	0.0183	0.0934	175
152	80	98	0.0238	0.108	175
153	80	99	0.0454	0.206	200
154	92	100	0.0648	0.295	175
155	94	100	0.0178	0.058	175

Table 4.11. IEEE 118-bus's transmission line data (cont'd)

Line No.	From Bus	To Bus	R (pu)	X (pu)	Flow Limit (MW)
156	95	96	0.0171	0.0547	175
157	96	97	0.0173	0.0885	175
158	98	100	0.0397	0.179	175
159	99	100	0.018	0.0813	175
160	100	101	0.0277	0.1262	175
161	92	102	0.0123	0.0559	175
162	101	102	0.0246	0.112	175
163	100	103	0.016	0.0525	500
164	100	104	0.0451	0.204	175
165	103	104	0.0466	0.1584	175
166	103	105	0.0535	0.1625	175
167	100	106	0.0605	0.229	175
168	104	105	0.00994	0.0378	175
169	105	106	0.014	0.0547	175
170	105	107	0.053	0.183	175
171	105	108	0.0261	0.0703	175
172	106	107	0.053	0.183	175
173	108	109	0.0105	0.0288	175
174	103	110	0.03906	0.1813	175
175	109	110	0.0278	0.0762	175
176	110	111	0.022	0.0755	175
177	110	112	0.0247	0.064	175
178	17	113	0.00913	0.0301	175
179	32	113	0.0615	0.203	500
180	32	114	0.0135	0.0612	175
181	27	115	0.0164	0.0741	175
182	114	115	0.0023	0.0104	175
183	68	116	0.00034	0.00405	500
184	12	117	0.0329	0.14	175
185	75	118	0.0145	0.0481	175
186	76	118	0.0164	0.0544	175

Table 4.12. Total PV installation capabilities and their locations

Areas	Locations	Case 1	Case 2
A	bus 5, 11, 14, 16	176 MW	290 MW
B	bus 17, 20, 23, 29	174 MW	261 MW
C	bus 33, 35, 37, 41	145 MW	252 MW
D	bus 45, 48, 53, 67	126 MW	232 MW
E	bus 75, 83, 94, 98	101 MW	227 MW

Table 4.13. Bus load distribution profile for IEEE 118-bus

Load	At Bus	Load Ratio
1	1	1.450281
2	2	0.568701
3	3	1.109007
4	4	0.853185
5	6	1.478676
6	7	0.540306
7	11	1.990587
8	12	1.336434
9	13	0.966765
10	14	0.398064
11	15	2.559288
12	16	0.710943
13	17	0.312879
14	18	1.706103
15	19	1.279644
16	20	0.511911
17	21	0.398064
18	22	0.284484
19	23	0.199032
20	27	1.76316
21	28	0.483516
22	29	0.682548
23	31	1.222854

Table 4.13. Bus load distribution profile (cont'd)

Load	At Bus	Load Ratio
24	32	1.677708
25	33	0.654153
26	34	1.677708
27	35	0.93837
28	36	0.88158
29	39	0.723265
30	40	0.535752
31	41	0.991141
32	42	0.991141
33	43	0.482177
34	44	0.428602
35	45	1.419743
36	46	0.750053
37	47	0.910779
38	48	0.535752
39	49	2.330522
40	50	0.455389
41	51	0.455389
42	52	0.482177
43	53	0.616115
44	54	3.026999
45	55	1.687619
46	56	2.250159
47	57	0.321451
48	58	0.321451
49	59	7.420166
50	60	2.089433
51	62	2.062646
52	66	1.044717
53	67	0.750053
54	70	1.767982

Table 4.13. Bus load distribution profile (cont'd)

Load	At Bus	Load Ratio
55	74	1.821557
56	75	1.259017
57	76	1.821557
58	77	1.634044
59	78	1.90192
60	79	1.044717
61	80	3.482389
62	82	1.446531
63	83	0.535752
64	84	0.294664
65	85	0.642903
66	86	0.56254
67	88	1.285805
68	90	2.089433
69	92	1.741194
70	93	0.321451
71	94	0.803628
72	95	1.125079
73	96	1.017929
74	97	0.401814
75	98	0.910779
76	100	0.991141
77	101	0.589327
78	102	0.133938
79	103	0.616115
80	104	1.017929
81	105	0.830416
82	106	1.151867
83	107	0.750053
84	108	0.053575
85	109	0.214301

Table 4.13. Bus load distribution profile (cont'd)

Load	At Bus	Load Ratio
86	110	1.044717
87	112	0.66969
88	114	0.227427
89	115	0.625491
90	117	0.568701
91	118	0.883991

Figure 4.17 (a)-(d) depicts the distance *d* between the bounds of RDF for two cases with maximum prediction errors of $\sigma_{PV} = 0\%$, 10%, 30%, and 30% with contingency scenario, respectively. For the contingency case, the outage of one line is assumed at the line between buses 69 and 70, and that between bus 100 and 103. The characteristics of indicator *d* are similar to 6-bus system results. When the forecast is more erroneous, *d* is smaller, where the system operation may be less reliable and secure.

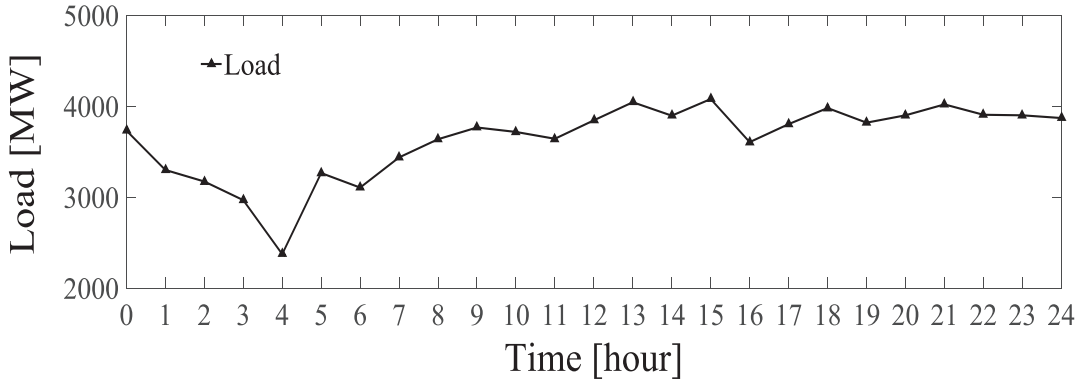

(a) Hourly total load data

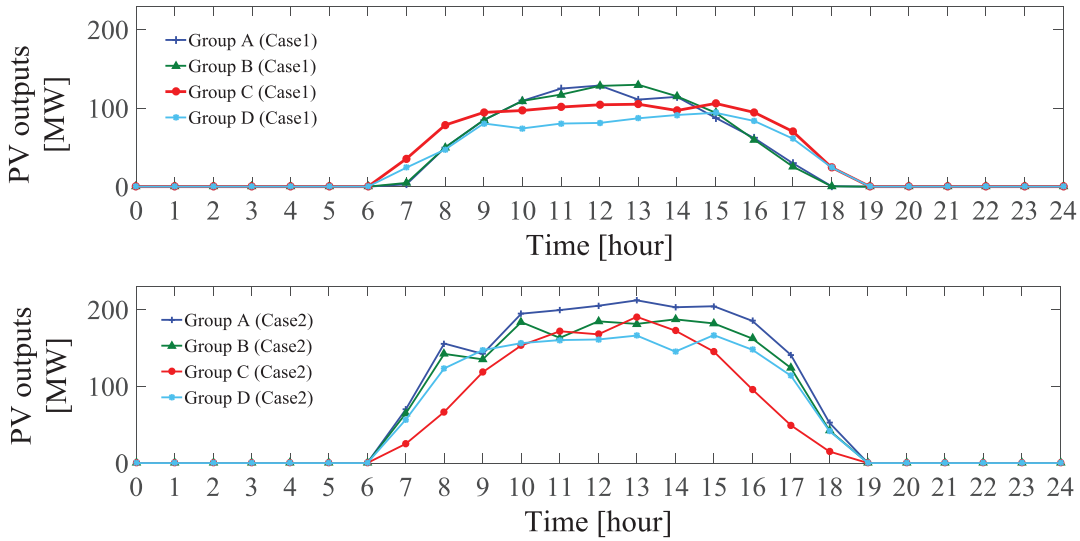

(b) Hourly total PV data

Figure 4.16. Hourly total load and PV data for modified IEEE 118 bus

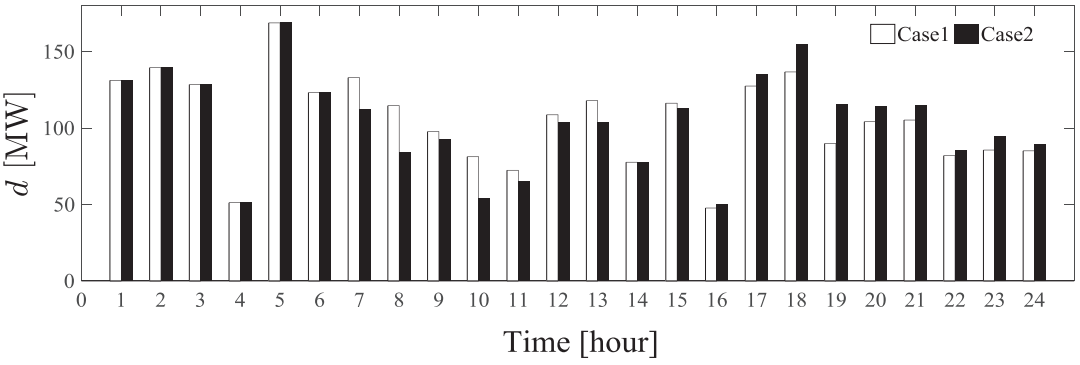

(a) $\sigma_{PV} = 0\%, \sigma_D = 3\%$

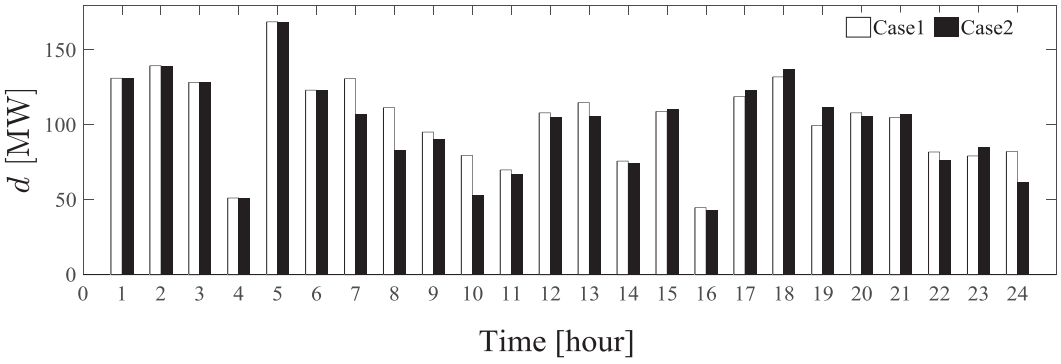

(b) $\sigma_{PV} = 10\%, \sigma_D = 3\%$

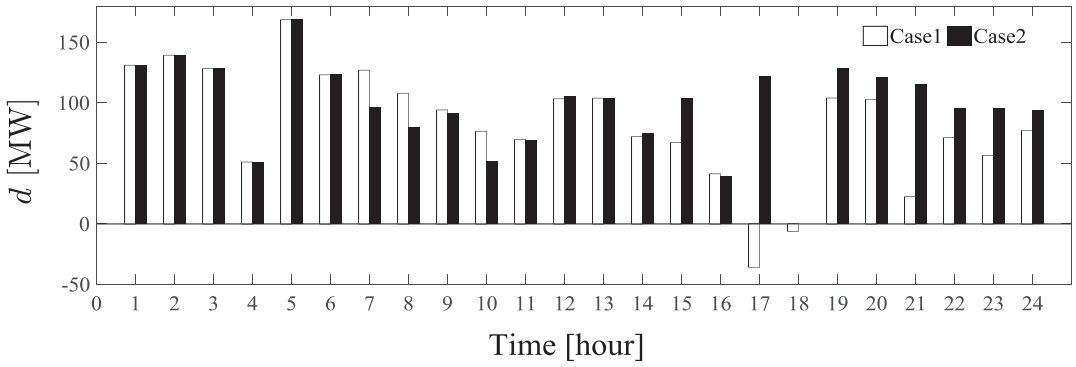

(c) $\sigma_{PV} = 30\%, \sigma_D = 3\%$

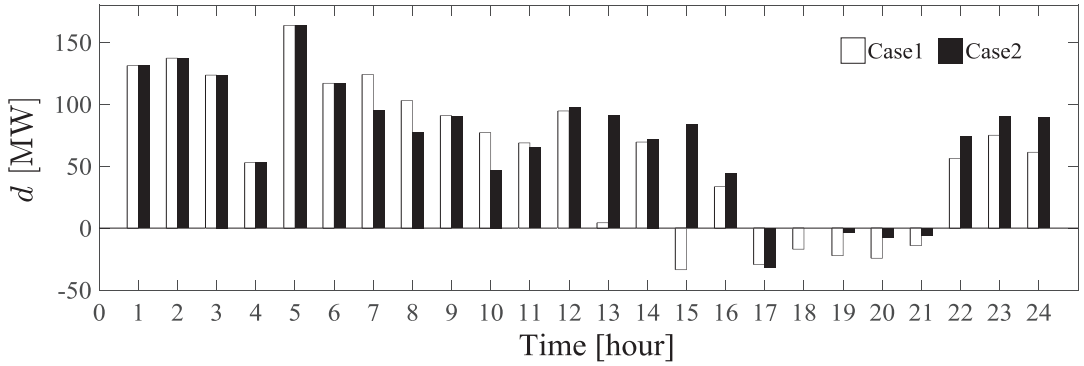

(d) $\sigma_{PV} = 30\%, \sigma_D = 3\%$ and N-1 contingency

Figure 4.17. Size of feasibility region *d* measured in MW for modified IEEE 118-bus; Negative values indicate possible power mismatch in the worst case

Negative *d* is observed at around 17:00, when the RDF region shrinks and disappears. When *d* is too small, the operator may take action in advance, such as obtaining additional power supply, demand response, load shedding, *etc*. Such actions may be prepared in the system planning.

4.4.9. Computational Burden

CPU times for proposed optimization method are listed in Tables 4.14 and 4.15. The simulations are carried out using Intel Core i7 2.20GHz, 8GB of RAM Memory. The proposed method is implemented using Matlab/Simulink optimization toolbox "intlinprog".

Table 4.14 CPU time computation for six-bus and IEEE 118-bus models

	Case	CPU Time (s)	
		6-bus	118-bus
$\sigma_{PV} = 0\%,\ \sigma_D = 3\%$	1	26.4	466.9
	2	26.9	516.3
$\sigma_{PV} = 10\%,\ \sigma_D = 3\%$	1	29.5	471.4
	2	29.0	493.1
$\sigma_{PV} = 30\%,\ \sigma_D = 3\%$	1	29.1	411.1
	2	28.9	542.2
$\sigma_{PV} = 30\%,\ \sigma_D = 3\%$ with contingency	1	31.0	1313
	2	32.0	2437

Table 4.15 Calculation of CPU time for IEEE 14-bus and IEEE 30-bus power system models

Power System Model	Case		CPU Time (s)
IEEE 14-bus	1	$\sigma_{PV} = 0\%,\ \sigma_D = 0\%$	36.82
	2	$\sigma_{PV} = 10\%,\ \sigma_D = 3\%$	36.77
	3	$\sigma_{PV} = 30\%,\ \sigma_D = 5\%$	35.33
	4	Case 3 with contingency	40.44
IEEE 30-bus	1	$\sigma_{PV} = 0\%,\ \sigma_D = 3\%$	77.61
	2	$\sigma_{PV} = 10\%,\ \sigma_D = 3\%$	76.70
	3	$\sigma_{PV} = 30\%,\ \sigma_D = 3\%$	77.29
	4	Case 3 with contingency	91.08

4.5. Concluding Remarks

This chapter proposes a new method based on bi-level optimization to compute the size of the worst case feasible region under uncertainties. Dynamic economic dispatch with uncertainties of PV forecast are investigated, where the security assessment of 24-hour system operation is carried out. The larger power system model is used to verify the efficacy of the proposed approach, the more CPU time is exhausted to obtain the optimal solution for a robust power system security problem.

It has been confirmed that the method is advantageous to analyze the feasibility of system operation, the degree of system reliability against uncertainties.

CHAPTER 5 : CONCLUSIONS AND FUTURE WORKS

5.1. Conclusions

In this study, a new formulation and approach to computing the security region to deal with uncertainties are proposed. The problem formulations are composed of deterministic and linear constraints methods. DC power flow is used to show the efficacy of the proposed approach. Two types of security regions for static operating point and dynamic transition of system operation are proposed, which are robust static security (RSS) and robust dynamic feasible (RDF) regions, respectively. The main conclusions of this thesis can be summarized as follows:

Chapter 2 describes basic concept and definition of power system security, including the brief overview of conventional methods. The concept of Robust Power System Security dealing with uncertainties is described as an introduction to the following chapters.

Chapter 3 presents a new approach for RSS problem applied to static economic dispatch. The proposed method is to obtain upper and lower bounds of security region. The difference between the bounds indicates the diameter of security region, which can be used as a security measure. Linear programming (LP) is employed to solve the RSS problem. The effectiveness of the proposed method is demonstrated taking into account uncertainties of PV generations.

Finally, Chapter 4 provides the extension of RSS problem. In order to measure the security region in dynamic power system operation circumstances, RDF region is defined. A bi-level optimization problem is formulated to monitor RDF region. Then, the problem is linearized and transformed into mixed integer linear programming (MILP) problem, which can be effectively solved. The proposed approach is examined by six-bus, IEEE 14-bus, IEEE 30-bus, and IEEE 118-bus standard models taking into account all dynamic factors in power system operation. It is shown that the method clearly indicates dangerous operating hours in a 24-hour system operation.

5.2. Future Works

The use of the alternative approach based on primal-dual transformation in [69] from the point of view of computational efficiency seems effective to decrease the number of binary variables. Other necessary examinations include effective treatment of N-k contingencies such as tighter treatment of security criteria in [59]–[61], [19], [20]. Improvement of computational techniques concerned with contingencies is important to subject. Application of faster solution such as decomposition method is expected to solve the problem for large scale system.

REFERENCES

[1] T. E. Dy Liacco, "System security: the computer's role," *IEEE Spectrum*, vol. 15, no. 6, pp. 43-50, Jun. 1978.

[2] B. Stott and E. Hobson, "Power system security control calculations using linear programming, Part 1 & Part 2*," IEEE Trans. Power App. Syst.*, vol. PAS-97, no. 5, pp. 1713-1731, Sep./Oct. 1978.

[3] M. H. Banakar and F. D. Galiana, "Power system security corridors concept and computation," *IEEE Trans. Power App. Syst.*, vol. PAS-100, no. 11, pp. 4524-4532, Nov. 1981.

[4] B. Stott and J.L. Marinho, "Linear programming for power-system network security applications," *IEEE Trans. Power App. Syst.*, vol. PAS-98, no. 3, pp. 837-848, May 1979.

[5] J. L. Carpentier and G. Cotto, "Modern concepts for security control in electric power system," No. R-102-01, in *Proc. of CIGRE-IFAC Symp. on Control Applications to Power System Security*, Florence, Italy; Sept. 1983;

[6] R. C. Burchett and H. H. Happ, "Large scale security dispatching: an exact model," *IEEE Trans. Power App. Syst.*, vol. PER-3, no. 9, pp. 32-33, Sept. 1983.

[7] B. Stott, O. Alsac, and A.J. Monticelli, "Security analysis and optimization," in *Proc. of the IEEE*, Dec. 1987, pp. 1623-1644.

[8] A. Monticelli, M. V. F. Pereira, and S. Granville, "Security-constrained optimal power flow with post-contingency corrective rescheduling," *IEEE Trans. Power Syst.*, vol. 2, no. 1, pp. 175-180, Feb. 1987.

[9] Y. Yuan, J. Kubokawa, and H. Sasaki, "A solution of optimal power flow with multi contingency transient stability constraints," *IEEE Trans. Power Syst.*, vol. 18, no. 3, pp. 1094-1102, Aug. 2003.

[10] G. Hug-Glanzmann and G. Andersson, "N-1 security in optimal power flow control applied to limited areas," *IET Gen. Trans. Dist,* vol. 3, no. 2, pp. 206-215, Feb. 2009.

[11] G. D. Irisarri and A. M. Sasson, "An automatic contingency selection method for on-line security analysis," *IEEE Trans. Power App. Syst*., vol. PAS-100, no. 4, pp. 1838-1844, April 1981.

[12] K. Nara, K. Tanaka, H. Kodama, R. R. Shoults, M. S. Chen, P. V. Olinda, and D. Bertagnolli, "On-line contingency selection algorithm for voltage security analysis," *IEEE Trans. Power App. Syst.*, vol. PAS-104, no. 4, pp. 846-856, July 1985.

[13] N. Yorino, E. E. El-Araby, H. Sasaki, and S. Harada, "A new formulation for FACTS allocation for security enhancement against voltage collapse," *IEEE Trans. on Power Syst.*, vol. 18, no. 1, pp. 3-10, Feb. 2003.

[14] H. Sun, D.C. Yu, and Y. Xie, "Flexible steady-state security region of power system with uncertain load demand and soft security limits," in *Proc. of IEEE Power Engineering Society Summer Meeting*, Seattle, USA, 2000.

[15] M. Ni, J. D. McCalley, V. Vittal, and T. Tayyib, "Online risk-based security assessment," *IEEE Trans. on Power Syst.*, vol. 18, no. 1, pp. 258-265, Feb. 2003.

[16] E.A. Al-Ammar and M.A. El-Kady, "Application of operating security regions in power systems," in *Proc. 2010 of IEEE PES Trans. Dist. Conf. & Expo*, New Orleans, USA, April 2010.

[17] F. Bouffard, F. D. Galiana, and A. J. Conejo, "Market-clearing with stochastic security, Part 1 & Part 2," *IEEE Trans. Power Syst.*, vol. 20, no. 4, pp. 1818-1835, Nov. 2005.

[18] Q. Wang, J. D. McCalley, T. Zheng, and E. Litvinov, "A computational strategy to solve preventive risk-based security-constrained opf," *IEEE Trans. on Power Syst.*, vol. 28, no. 2, pp. 1094-1102, May 2013.

[19] A. Street, F. Oliveira, and J. M. Arroyo, "Contingency-constrained unit commitment with n-k security criterion: a robust optimization approach," *IEEE Trans. Power Syst.*, vol. 26, no. 3, pp. 1581-1590, Aug. 2011.

[20] A. Moreira, A. Street, and J. M. Arroyo, "An adjustable robust optimization approach for contingency-constrained transmission expansion planning," *IEEE Trans. Power Syst.*, vol. 30, no. 4, pp. 2013–2022, Jul. 2015.

[21] D. Bertsimas, E. Litvinov, X. A. Sun, J. Zhao, and T. Zheng, "Adaptive robust optimization for the security constrained unit commitment problem," *IEEE Trans. Power Syst.*, vol. 28, no. 1, pp. 52-63, Feb. 2013.

[22] A. Lorca, and X. A. Sun, "Adaptive robust optimization with dynamic uncertainty sets for multi-period economic dispatch under significant wind," *IEEE Trans. Power Syst.*, vol. 30, no. 4, pp. 1702–1713, Jul. 2015.

[23] F. Capitanescu, S. Fliscounakis, P. Panciatici, and L. Wehenkel, "Cautious operation planning under uncertainties," *IEEE Trans. Power Syst.*, vol. 27, no. 4, pp. 1859-1869, Nov. 2012.

[24] F. Capitanescu and L. Wehenkel, "Computation of worst operation scenarios under uncertainty of static security management," *IEEE Trans. Power Syst.*, vol. 28, no. 2, pp. 1697-1705, May 2013.

[25] J. Warrington, C. Hohl, P. J. Goulart, and M. Morari, "Rolling unit commitment and dispatch with multi-stage recourse policies for heterogeneous devices," *IEEE Trans. Power Syst.*, vol. 31, no. 1, pp. 187-197, Nov. 2016.

[26] O. Alizadeh-Mousavi and M. Nick A, "Stochastic security constrained unit commitment with variable-speed pumped-storage hydropower plants," in *Proc. of 19th Power System Computation Conference (PSCC)*, Jun. 2016, pp.1-6.

[27] E. Lannoye, D. Flynn, and M. O'Malley, "Evaluation of power system flexibility," *IEEE Trans. Power Syst.*, vol. 27, no. 2, pp. 922-931, May 2012.

[28] J. Zhao, T. Zheng, and E. Litvinov, "A unified framework for defining and measuring flexibility in power system," *IEEE Trans. Power Syst.*, vol. 31, no. 1, pp. 339-347, Jan. 2016.

[29] M. A. Bucher, S. Chatzivasileiadis, and G. Andersson "Managing flexibility in multi-area power systems," *IEEE Trans. Power Syst.*, vol. 31, no. 2, pp. 1218–1226, Mar. 2016.

[30] J. Zhao, T. Zheng, and E. Litvinov, "Variable resource dispatch through do-not-exceed limit," *IEEE Trans. Power Syst.*, vol. 30, no. 2, pp. 820–828, Mar. 2015.

[31] A. S. Korad and K. W. Hedman, "Enhancement of do-not-exceed limit with robust corrective topology control," *IEEE Trans. Power Syst.*, vol. 31, no. 3, pp. 1889–1899, May 2016.

[32] W. Wei, F. Liu, and S. Mei, "Dispatchable region of the variable wind generation," *IEEE Trans. Power Syst.*, vol. 30, no. 5, pp. 2755–2765, Sept. 2015.

[33] A. A. Jahromi and F. Bouffard, "On the loadability sets of power systems–Part I: Characterization, &–Part II: Minimal Representations," *IEEE Trans. Power Syst.*, vol. 32, no. 1, pp. 137-156, Jan. 2017.

[34] Y. Okumoto, N. Yorino, Y. Zoka, Y. Sasaki, T. Yamanaka, and T. Akiyoshi, "An application of robust power system security to power system operation for high-penetration of PV," in *Proc. of 2012 3rd IEEE PES International Conference and Exhibition on Innovative Smart Grid Technologies Conf.*, Oct. 2012, pp. 1-7.

[35] N. Yorino, Y. Sasaki, E.P. Hristov, Y. Zoka, and Y. Okumoto, "Dynamic load dispatch for power system robust security against uncertainties," in *Proc. of 2013 IREP Symp.*, Crete, Greece, Aug. 2013, pp. 1-17.

[36] N. Yorino, E. Popov, Y. Zoka, Y. Sasaki, and H. Sugihara, "An application of critical trajectory method to bcu problem for transient stability studies," *IEEE Trans Power Syst.*, vol. 28, no. 4, pp. 4237-4244, Nov. 2013.

[37] N. Yorino, A. Priyadi, H. Kakui, and M. Takeshita, "A new method for obtaining critical clearing time for transient stability," *IEEE Trans. Power Syst.*, vol. 25, no. 3, pp. 1620-1626, Aug. 2010.

[38] A. Priyadi, N. Yorino, M. Tanaka, T. Fujiwara, H. Kakui, and M. Takeshita, "A direct method for obtaining critical clearing time for transient stability using critical generator conditions," *European Trans. on Electrical Power*, vol. 22, no. 5, pp. 674-687, Jul. 2012.

[39] E. Lannoye, D. Flynn, and M. O'Malley, "Evaluation of power system flexibility," *IEEE Trans. Power Syst.*, vol. 27, no. 2, pp. 922-931, May 2012.

[40] J. Zhao, T. Zheng, and E. Litvinov, "A unified framework for defining and measuring flexibility in power system," *IEEE Trans. Power Syst.*, vol. 31, no. 1, pp. 339-347, Jan. 2016.

[41] M. A. Bucher, S. Chatzivasileiadis, and G. Andersson "Managing flexibility in multi-area power systems," *IEEE Trans. Power Syst.*, vol. 31, no. 2, pp. 1218–1226, Mar. 2016.

[42] J. Zhao, T. Zheng, and E. Litvinov, "Variable resource dispatch through do-not-exceed limit," *IEEE Trans. Power Syst.*, vol. 30, no. 2, pp. 820–828, Mar. 2015.

[43] A. S. Korad and K. W. Hedman, "Enhancement of do-not-exceed limit with robust corrective topology control," *IEEE Trans. Power Syst.*, vol. 31, no. 3, pp. 1889–1899, May 2016.

[44] Y. Sasaki, N. Yorino, and Y. Zoka, "Probabilistic economic load dispatch applied to a micro-ems controller," in *Proc. of 19th Power System Computation Conference (PSCC)*, Jun. 2016, pp.1-6.

[45] H.M. Hafiz, N. Yorino, Y. Sasaki, and Y. Zoka, "Feasible operation region for dynamic economic dispatch and reserve monitoring," *European Trans. on Electrical Power*, vol. 22, no. 7, pp. 924-936, Oct. 2012.

[46] N. Yorino, H. M. Hafiz, Y. Sasaki, and Y. Zoka, "High-speed real-time dynamic economic load dispatch," *IEEE Trans. Power Syst.*, vol. 27, no. 2, pp. 621-630, May 2012.

[47] T.E. Dy Liacco, "The adaptive reliability control system," *IEEE Trans. Power App. Syst.*, vol. PAS-86, no. 5, pp. 517–531, May 1967.

[48] F. F. Wu, "Real-time network security monitoring, assessment and optimization," *Electrical Power & Energy Systems*, vol. 10, no. 2, pp. 83–100, April 1988.

[49] R. J. Ringlee, Chmn, P. Albrecht, R. N. Allan, M. P. Bhavaraju, R. Billinton, R. Ludorf, B. K. LeReverend, E. Neudorf, M. G. Lauby, P. R. S. Kuruganty, M. F. McCoy, T. C. Mielnik, N. S. Rau, B. Silverstein. C. Singh, J. A. Stratton, "Bulk power system reliability criteria and indices trends and future needs," *IEEE Trans. Power App. Syst.*, vol. 9, no. 1, pp. 181–188, Feb. 1994.

[50] R. J. Marceau and J. Endrenyi, Chairmen, "Power system security assessment: a position paper," *Electra*, no. 175, pp. 48-78, Dec. 1997.

[51] J. Endrenyi and W. Wellssow, "Power system reliability in terms of the system's operating states," in *Proc. of the IEEE Power Tech Conference*, Porto, Portugal, Sept. 2001.

[52] N. Yorino, Y. Okumoto, T. Suizu, "Robust power system security : necessity of new concept for power system security to deal with uncertainties of renewable energy generations," EPCC workshop, Jun. 2013. [Online]. Available: http://www.epcc-workshop.net/assets/downloads/yorino-prsentation-robust-power-system.pdf.

[53] N. Yorino, Y. Sasaki, S. Fujita, Y. Okumoto, and Y. Zoka, "Issues for power system operation for future renewable energy penetration: robust power system security," *Electrical Engineering in Japan*, vol. 182, no. 1, pp. 30-38, Jan. 2013. *Translated from IEEJ Trans. on Power and Energy*, vol. 131, no.8, pp. 670-676, Aug. 2011.

[54] Y. Okumoto, N. Yorino, Y. Zoka, Y. Sasaki, S. Fujita, and T. Yamanaka, "A concept of robust power system security and its application under renewable energy sources penetration," in *Proc. of 2012 IEEE PES Innovative Smart Grid Technologies Conf.*, Jan. 2012, pp. 1-7.

[55] N. Yorino, M. Abdillah, T. Isoya, Y. Sasaki, and Y. Zoka, "A new method of evaluating robust power system security against uncertainties," *IEEJ Trans. on Elect. and Electron. Eng.*, vol. 10, no. 6, pp. 636-643, Nov. 2015.

[56] N. Yorino, M. Abdillah, Y. Sasaki, and Y. Zoka, "Robust power system security assessment under uncertainties using bi-level optimization," *IEEE Trans. Power Syst.*, vol. PP, no. 99, pp. 1-1, April 2017. (**To appear**)

[57] N. Yorino, M. Abdillah, Y. Sasaki, and Y. Zoka, **"**A Method for evaluating robust power system security against uncertainties**,"** in *Proc. of 2016 International Seminar on Intelligent Technology and Its Appalications (ISITIA)***,** July 2016, pp. 497-502.

[58] N. Yorino, M. Abdillah, and Y. Sasaki, "Monitoring the region of robust power system security against uncertainties**,"** in *Proc. of The 2016 IEEE PES Innovative Smart Grid Technologies (ISGT)***,** Dec. 2016, pp. 1213-1218.

[59] A. L. Motto, J. M. Arroyo, and F. D. Galiana, "A mixed integer LP procedure for the analysis of electric grid security under disruptive threat," *IEEE Trans. Power Syst.*, vol. 20, no. 3, pp. 1357-1365, Aug. 2005.

[60] J. M. Arroyo, and F. D. Galiana, "On the solution of the bilevel programming formulation of the terrorist threat problem," *IEEE Trans. Power Syst.*, vol. 20, no. 2, pp. 789–797, May 2005.

[61] J. Salmeron, K. Wood, and R. Baldick, "Worst-case interdiction analysis of large-scale electric power grids," *IEEE Trans. Power Syst.*, vol. 24, no. 1, pp. 96–103, Feb. 2009.

[62] T. Kim, S. J. Wright, D. Bienstock, and S. Harnett, "Analyzing vulnerability of power systems with continuous optimization formulations", *IEEE Trans. Power Syst.*, vol. 3, no. 3, pp. 132–146, Sept. 2016.

[63] H. Wu, M. Shahidehpour, and M.E. Khodayar, "Hourly demand response in day-ahead scheduling considering generating unit ramping cost", *IEEE Trans. Power Syst.*, vol. 28, no. 3, pp. 2446-2454, Aug. 2013.

[64] H. Wu, X. Guan, Q. Zhai, F. Gao, and Y. Yang, "Security-constrained generation scheduling with feasible energy delivery," in *Proc. of 2009 IEEE Power Eng. Soc. General Meeting*, Calgary, AB, Canada, Jul. 2009, pp.1-6.

[65] National renewable energy laboratory (NREL), data and resources [Online]. Available:http://www.nrel.gov/electricity/transmission/data_resources.html.

[66] A. Lotfjou, M. Shahidehpour, Y. Fu, Z. Li, "Security constrained unit commitment with AC/DC transmission systems," *IEEE Trans. Power Syst.*, vol. 25, no. 1, pp. 531-542, Feb. 2010.

[67] R. R. Gaddam, A. Jain, L. Belede, A PSO based smart unit commitment strategy for power systems including solar energy" in *Proc. of Seventh International Conference on Bio-Inspired Computing: Theories and Applications (BIC-TA 2012)*, *Advances in Intelligent Systems and Computing*, Dec. 2013, pp. 531-542.

[68] IEEE 118-Bus System, llinois institute of technology [Online]. Available: motor.ece.iit.edu/data.

[69] J. M. Arroyo. "Bilevel programming applied to power system vulnerability analysis under multiple contingencies," *IET Generation, Transmission & Distribution*, vol. 4, no. 2, pp. 178-190, Feb. 2010.

[70] C. Audet, P. Hansen, B. Jaumard, and G. Savard, "Links between linear bilevel and mixed 0–1 programming problems," *Journal of Optimization Theory and Applications*, vol. 93, no. 2, pp. 273-300, May 1997.

APPENDIX

A. Solution of Region Size Problem for RSS

Original problem (4.18) after linearization may be rewritten as the linear bi-level optimization problem as follows.

$$\bar{\alpha}_{RSS} = \min_{u,p}\{c^T u\} \tag{A.1}$$

Subject to

$$Ap + Bu \le b \tag{A.2}$$

$$u \in \arg\max_{u}\left\{c^T u\right\} \tag{A.3}$$

Subject to

$$Ap + Bu \le b \tag{A.4}$$

The lower-level problem (A.3)-(A.4) is transformed by using KKT necessary optimality condition into a set of constraints in the upper level problem to form a single-level problem. A binary vector and sufficiently large value L are introduced to treat the non-linear complementary slackness condition to obtain its equivalent linear form. Thus, the original bi-level problem (A.1)-(A.4) is converted into an equivalent single-level optimization problem (A.5)-(A.11). The bi-level optimization approach in details is provided in [70].

$$\bar{\alpha}_{RSS} = \min_{u,p}\{c^T u\} \tag{A.5}$$

Subject to

$$Ap + Bu \le b \tag{A.6}$$

$$\begin{bmatrix} u^T & \lambda^T \end{bmatrix} \le L \begin{bmatrix} u_{bin}^T & \lambda_{bin}^T \end{bmatrix} \tag{A.7}$$

$$\begin{bmatrix} c - A^T\lambda \\ b - Bp - Au \end{bmatrix} \le L \begin{bmatrix} 1 - u_{bin} \\ 1 - \lambda_{bin} \end{bmatrix} \tag{A.8}$$

$$c^T \le \lambda^T A \tag{A.9}$$

$$\lambda \ge 0 \tag{A.10}$$

$$u_{bin}, \lambda_{bin} \in \{0,1\} \tag{A.11}$$

L: Large value (L=50,000 is used.)

The similar procedure may be applied to the problem (4.19) in order to obtain the equivalent problem as follows:

$$\underline{\alpha}_{RSS} = \max_{u,p} \{c^T u\} \tag{A.12}$$

Subject to constraints (A.6)-(A.11).

The obtained MILP can be solved by a commercial software package such as MATLAB/SIMULINK Optimization Toolbox.